

ChemComm

Accepted Manuscript



This is an *Accepted Manuscript*, which has been through the Royal Society of Chemistry peer review process and has been accepted for publication.

Accepted Manuscripts are published online shortly after acceptance, before technical editing, formatting and proof reading. Using this free service, authors can make their results available to the community, in citable form, before we publish the edited article. We will replace this *Accepted Manuscript* with the edited and formatted *Advance Article* as soon as it is available.

You can find more information about *Accepted Manuscripts* in the [Information for Authors](#).

Please note that technical editing may introduce minor changes to the text and/or graphics, which may alter content. The journal's standard [Terms & Conditions](#) and the [Ethical guidelines](#) still apply. In no event shall the Royal Society of Chemistry be held responsible for any errors or omissions in this *Accepted Manuscript* or any consequences arising from the use of any information it contains.

ARTICLE

Stimuli-responsive Cancer Therapy based on Nanoparticles

Cite this: DOI: 10.1039/x0xx00000x

Jing Yu,^a Xin Chu^a and Yanglong Hou^{*a}

Received 00th January 2012,
Accepted 00th January 2012

DOI: 10.1039/x0xx00000x

www.rsc.org/

Nanoparticles (NPs) have been well investigated for cancer therapy recently. Among them, those that are responsive to internal or external stimuli are promising due to their flexibility. In this feature article, we provide an overview on stimuli-sensitive cancer therapy, using pH-, reduction-sensitive NPs as well as light-, magnetic field-responsive NPs.

1. Introduction

During the past decades, cancer has been ranked the second leading cause of death followed by cardiovascular diseases.¹ The battle with cancer, mainly treated with surgical resection, radiation therapy and chemotherapy, however, is still difficult with pronounced long-standing side effects, due to the similarity of cancerous cells to healthy human cells. Killing the diseased parts with less consequence on normal ones is of great significance. To achieve this purpose, finding differences between healthy and cancerous cells and realizing tumor-specific targeting is the key point in the process of eradicating cancer.

In fact, tumor blood vessels usually have more porous structures compared with normal blood vessels, with pore diameters commonly vary from 100 to 780 nm.² Nanoparticles (NPs), with diameter usually less than 100 nm, can therefore pass through these pores. Moreover, lymphatic drainage in cancer is compromised, which contributes to the retention of NPs at the tumor site after intravenous administration. This phenomenon, which is called the enhanced permeability and retention (EPR) effect, has been utilized in passive tumor targeting. Based on this, NPs can be developed as carriers, and bring drugs to the infected spots rather than unexpected sites. On the other hand, some tumor cells overexpress specific receptors, while these receptors are lower expressed or even absent in normal cells. For example, folate receptor and transferrin receptor are overexpressed in many types of cancer cells, and HER2 protein overexpression occurs in 18–20% of breast cancer.³ By exploiting the flexibility of NPs' surface, some targeting moiety (e.g., folate,⁴ transferrin⁵), peptides (e.g. RGD⁶), affibody⁷, and antibodies⁸, are conjugated to NPs for the more efficient active tumor targeting. More interestingly, the internal environment at tumorous tissue is slightly different

from normal part. Usually, the pH value is lower and reduction potential is different. Also, some enzymes such as matrix metalloproteinase are overexpressed in the extracellular environment of tumors. By developing their own reply to specific environment or conjugating with stimuli-sensitive molecules, NPs can therefore carefully be designed and engineered for stimuli-controlled cancer recognition based on these discrepancies.^{9–11} Despite these internal stimuli, “smart” systems response to external stimuli, such as light,¹² temperature,¹³ ultrasound,¹⁴ and magnetic field,^{15, 16} have also been exploited, with the advantage of spatial and temporal controlling the target sites. Owing to the high local concentration, reduced overall injection dose as well as reduced systematic toxicity, these stimuli-responsive NPs pave the way for the on-demand therapy.

In this feature article, we focus on recent advances in stimuli-sensitive therapy based on NPs. Both internal stimuli responsive NPs, including pH-, reduction-sensitive NPs and external inductive NPs, such as light- and magnetic field-controlled NPs will be covered.

2. pH-responsive therapy

Of all the stimuli so far studied, by exploiting the acidic environment of cancerous tissues, changing pH value is the most effective strategy in cancer therapy. It is well-documented that the pH value in tumor and inflammatory tissue is more acidic than in blood and normal tissue, due to the increased production and slow exportation of lactate and CO₂.¹ Moreover, other than mild acidic extracellular pH (pH_e) in tumor tissue, an even greater pH decrease can be found in intracellular compartments (pH_i), with endosomes and lysosomes are the most acidic organelles, where the pH values are 5.5 and 5.0, respectively. This phenomenon motivated dozens of work in

designing nanocarriers to respond to physiopathological pH changes and selectively trigger drug release in cancerous tissues. Basically, state-of-the-art pH-responsive systems are based on soft materials and inorganic solids. The former one can target tumor site based on weakly acidic pH_c and promote rapid drug release at endosomal/lysosomal pH within cells. According to a late review paper by Jiang et al, mechanisms for organic materials-based pH-sensitive targeting are mainly divided into shielding/deshielding mechanism, ligand exposure by pop-up mechanism, and ionization mechanism; while the controlled drug release is attribute to the destabilization or fusogenic ability of polymers.¹ However, in most of organic NPs-based pH-sensitive systems, NPs respond to pH values mildly with at least 2 pH units changes. Recently, a progress was made by Gao et al. by establishing a series of ultra pH-sensitive probes. These probes comprised of ultra pH-sensitive core, fluorophores and targeting unit, which render a sharp pH response with $\Delta pH_{10-90\%} < 0.25$. At blood pH value, the probes were present as self-assembled micelles with a complete silencing of the fluorophores due to the Homo-fluorescence resonance energy transfer. While at mild acidic pH_c or pH_i environment, the micelle dissociated, resulting in a 102-fold increase in fluorescence signals.¹⁷ In this chapter, we would like to comprehensively discuss the pH-responsive inorganic NPs.

Inorganic NPs-based pH-sensitive systems usually involve acid-labile linkers, which are in forms of either covalent bond, coordination bond, electrostatic force or intermolecular force (e.g. boronate ester,¹⁸ acetal,¹⁹ hydrazine,²⁰ amide,²¹ 1,3,5-triazaadamantane (TAA) group,²² and Schiff-base bond²³). Typically, they are used as a linker to conjugate gatekeeper on the carrier to avoid the early leakage of drugs before reaching the targeting sites, and being cleaved under acid environment via hydrolysis when being stimulated. For example, Liu et al. developed a rapid endosomal pH-responsive ensemble with Fe_3O_4 NPs being grafted on the pore openings of mesoporous silica NPs via TAA group. Such TAA linkers are stable in neutral/basic conditions, while can quickly be hydrolyzed into tri(aminomethyl) ethane when the pH is below 6.0 and release drugs encapsulated (Fig. 1a).²² The coordination bond between metal ions and functional group can also be utilized as a pH-responsive linker for triggered delivery. By forming a competition between metal ions and protons in the combination with the ligand, it can response to a smaller pH variation.^{24, 25}

Zn-loaded bovine serum albumin (Zn-BSA) NPs with drug loaded was applied as carriers for pH-responsive anticancer drug delivery through the cleavage of either the “Zn-BSA” or “Zn-drug” coordination bonding under designated pH conditions.²⁵ When the drugs are charged, they can directly bond to carriers through electrostatic force. By altering the environmental pH values, the attraction force would become repulsion force to trigger the drug release.²⁶ Alternatively, drugs containing aromatic group can conjugate with carrier through π - π interaction. This interaction can be weakened under the proton-rich environment and increase the release of drugs.²⁷⁻²⁹ By loading doxorubicine (DOX) within dopamine-plus-human serum albumin modified hollow iron oxide NPs (HIONPs-DOX), the Hou group realized the pH-triggered drug delivery to kill drug resistant cancer cells. Compared with free DOX, this probe is more likely to effectively uptaken by the multidrug resistant cells, and consequently more potent in cell killing (Fig. 1b).²⁹

Some inorganic NPs, such as manganese oxide,^{30, 31} manganese phosphate,⁴ iron oxide,³² zinc oxide,³³ calcium carbonate³⁴ and face centered cubic (fcc) FePt³⁵ are intrinsically pH-responsive, which are subject to acidic etching under acidic condition. Generally, they are usually with a hollow or porous structure, with drugs loaded in the cavity. By loading drugs on hollow manganese phosphate (HMP) NPs, we designed a pH-responsive drug delivery platform through the erosion of HMP NPs under an endosome/lysosome mimetic condition. With the conjugation of folate, NPs can be selectively uptaken by tumor cells, and delivered into endosome/lysosome, where they are cracked. This dissolution process triggers the release of drugs loaded and kills cells accordingly (Fig. 1c).⁴ pH-sensitive NPs can also regard as a gatekeeper, which can lead to a burst release when NPs dissolved at low pH condition.³³ Another interesting work reported by Sun et al. presented a controlled release of Fe in low pH solution by fcc FePt.³⁵ The released Fe catalyzes H_2O_2 decomposition into reactive oxygen species (ROS) within cells, causing fast oxidation and deterioration of cellular membranes. Moreover, it is well known that HCO_3^- can react with H^+ and generate CO_2 gas. When co-embedding HCO_3^- and drugs inside a nanoshell or polymer, and infiltrating them in an acid environment, the evolved CO_2 bubbles would cause the shell to rupture due to the increase in internal pressure, and as a result, promptly unload the encapsulated drug (Fig. 1d).^{36, 37}

ARTICLE

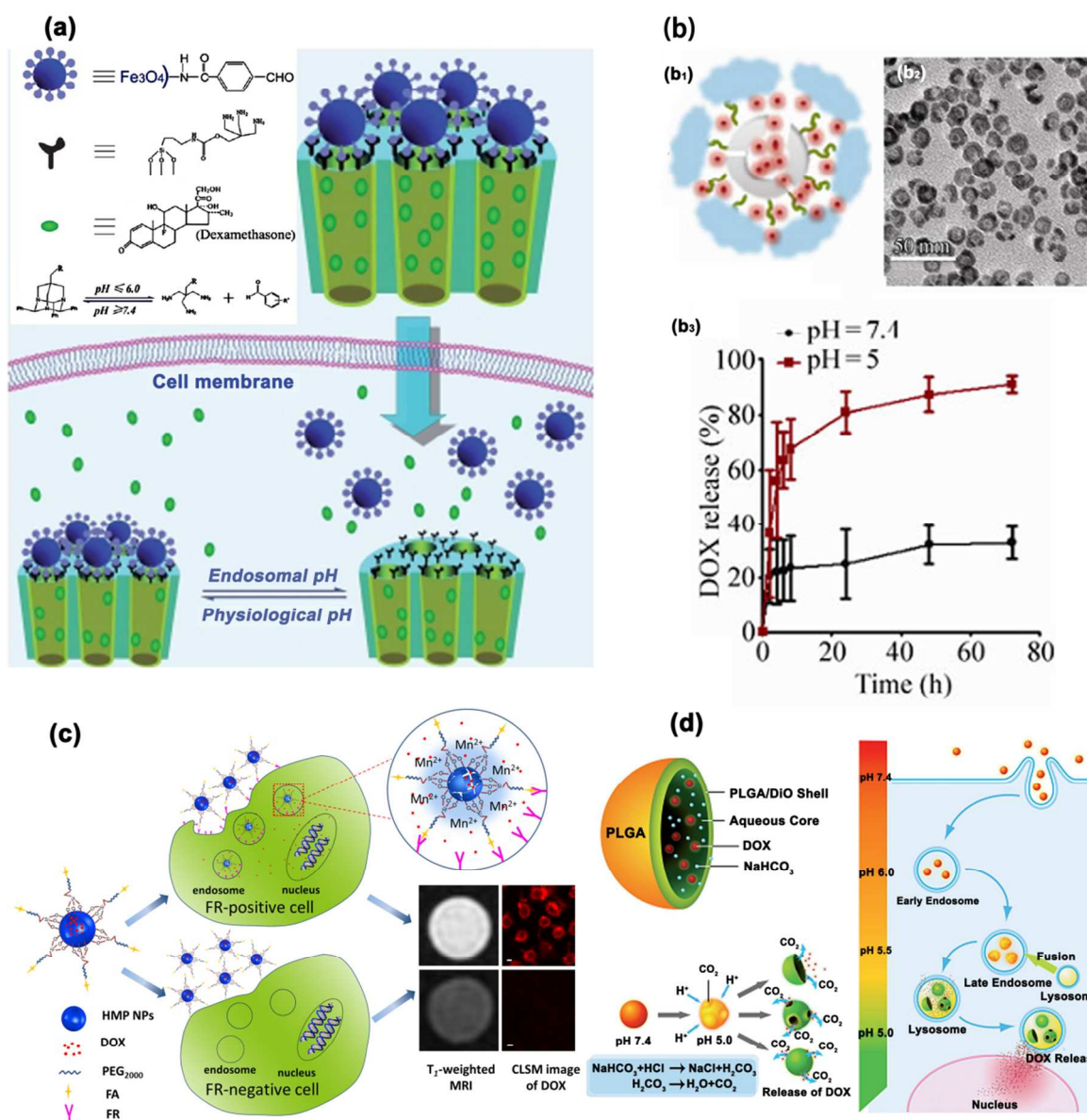


Fig. 1 (a) Schematic of the reversible pH-responsive Fe_3O_4 -capped mesoporous silica ensembles with an acid-labile triazaadamantane linker.²² Reproduced with permission from ref. 22. Copyright 2012 Royal Society of Chemistry. (b1) Schematic illustration and (b2) TEM image of HIONPs-based drug delivery system. (b3) Quantification of DOX release from HIONPs-DOX at pH 5 and pH 7.4.²⁹ Reproduced with permission from ref. 29. Copyright 2013 Tsinghua University Press and Springer-Verlag Berlin Heidelberg. (c) Schematic illustration of the concept for folate-mediated intracellular uptake of DOX-loaded HMP NPs for pH-selective MRI and drug delivery.⁴ Reproduced with permission from ref. 4. Copyright 2012 Tsinghua University Press and Springer-Verlag Berlin Heidelberg. (d) Schematic illustration of the structure of DOX-containing microsphere and the mechanism of pH-sensitive drug release (left), as well as the intracellular trafficking and releasing of the drug (right).³⁶ Reproduced with permission from ref. 36. Copyright 2011 WILEY-VCH Verlag GmbH & Co. KGaA, Weinheim.

3. Reduction-responsive therapy

Distinct differences in reduction potential between tumors and normal tissues have also been utilized as stimuli for cancer

therapy. Notably, some reductive enzymes, such as glutathione (GSH) is overexpressed in tumor microenvironments, reaching to at least 4-fold higher overexpression than that of normal tissue in mice. Meanwhile, there is a high GSH concentration gradient between extracellular and intracellular environment, which is $2\text{-}10\times 10^{-3}$ M intracellular, but $2\text{-}20$ μM in extracellular environment, leading to a site specific cleavage of reduction responsive linkers.^{38,39}

Disulfide linkages have been broadly applied in reduction-responsive drug delivery systems.⁴⁰ Conjugation of prodrugs, especially some hydrophobic or highly toxic drug on carriers by disulfide bonds, can enhance the effect of treatment by the on-demand bond cleavage. In general, a drug is linked to the carrier as an inactive prodrug via disulfide linker, and can be converted into the corresponding active parent drug by the bond cleaving process.⁴¹⁻⁴⁵ Perez et al. quenched both the fluorescence and cytotoxicity of DOX by covalently linking to folic acid with a disulfide linker. It is only when targeting to the folic acid positive cells and activating the linker in the presence of intracellular GSH that the fluorescence and cytotoxicity will increase (Fig. 2a).⁴⁴ However, this protocol has a shortcoming in which after the cleavage of the disulfide linker, the released compounds sometimes are not the active drug molecules but intermediates that need further conversion to active drugs.^{46,47} The more common applications of disulfide bond for controlled delivery are using disulfide cross-linked biocompatible polymers, including dextran,^{48,49} polypeptides,⁴⁵ polyester,⁵⁰ polyphosphoester,⁵¹ and polyurethanes⁵² with drugs physically loaded. Before reaching the target point, cross-linked micelle can efficiently prevent the drug leakage. When emerged in an intracellular space-mimicking environment, the enhanced reductive GSH would break the polymer by markedly

accelerating the cleavage of disulfide, and trigger the drug release.⁵² By using this method, Wang et al. designed a reduction-responsive micellar carrier for enhancing the efficiency in overcoming multidrug resistance of cancer cells. Compared with free drug, the carrier increased the influx but decreased the efflux of DOX by the shielding with either poly(ethylene glycol) or poly(ethyl ethylene phosphate), which lead to a high cellular retention of DOX. Based on the reduction of disulfide by intracellular GSH, the shell detached, and significantly accelerated the drug releasing (Fig. 2b).⁵¹ In addition, similar to pH-controlled delivery, gatekeepers can also be capped on porous NPs via the disulfide bond for the reduction-responsive delivery.^{53,54} The Yang group reported the fabrication of nanoreservoirs based on mesoporous silica NPs that are end-capped with collagen by disulfide bonds, which shows great potential for both cell-specific targeting and dithiothreitol controlled drug release (Fig. 2c).⁵⁴

Besides disulfide bonds, there are some other types reduction-responsive linkers, which are also candidates for the reduction-responsive delivery. Diselenide bond, which has a similar chemical properties but lower bond energies compared with disulfide bond, is able to fabricate more sensitive drug carriers under stimuli.⁴⁰ Zhang et al. confirmed this concept by cleaving the diselenide-bond even the final GSH concentration is as low as 0.1 mg/mL.⁵⁵ Another interesting reduction-responsive system was developed by Jo et al. by using trimethyl-locked benzoquinone, which can be transformed into lactone via intra-molecular cyclization under a two-electron reduction (Fig. 2d). It shows that about 52% of the encapsulated paclitaxel was released within 3 h in the presence of sodium dithionite while only 13% was released over 12 h in the absence of the reducing agent.¹⁰

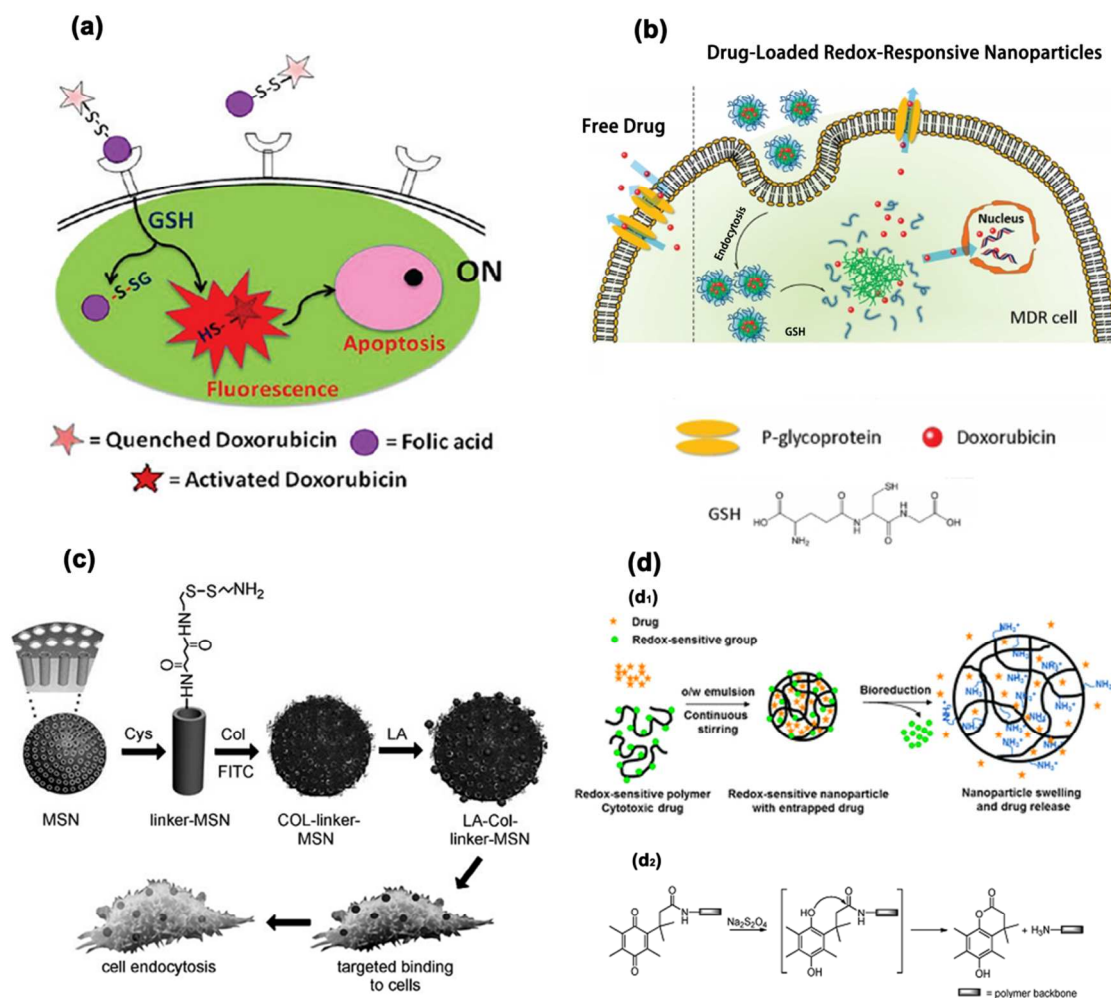


Fig. 2 (a) Schematic illustration of reduction-responsive DOX-conjugated folic acid in the extracellular milieu.⁴⁴ Reproduced with permission from ref. 44. Copyright 2011 American Chemical Society. (b) Schematic illustration of reduction-responsive NPs for overcoming multidrug resistance of cancer cells.⁵¹ Reproduced with permission from ref. 51. Copyright 2011 American Chemical Society. (c) Fabrication of a nanoreservoir based on a reduction-responsive mesoporous silica NPs for targeted drug delivery and cell uptake in situ.⁵⁴ Reproduced with permission from ref. 54. Copyright 2011 WILEY-VCH Verlag GmbH & Co. KGaA, Weinheim. (d1) Schematic illustration and (d2) chemical reduction of the reduction-sensitive polymers based on trimethyl-locked benzoquinone.¹⁰ Reproduced with permission from ref. 10. Copyright 2012 Royal Society of Chemistry.

4. Light-active therapy

Stimuli-responsive NPs discussed previously are normally excited by the internal environment, which have the advantages of self-controlled drug release and facile application in the clinical settings. On the other hand, another category of controlled therapy called external stimuli-responsive therapy, such as light-, ultrasound-, magnetic field- and heat-induced therapy, offer the merits of precision spatial, temporal as well as dose control over drug release through a remote apparatus, and can switch on and off of the drug release at will.⁵⁶ Among these external stimuli, light is the most flexible one to alter the site treated and the intensity applied. In this chapter, we will discuss the light-active therapy based on photothermal therapy (PTT), photodynamic therapy (PDT), light-triggered delivery and imaging-guided therapy.

4.1 Photothermal therapy

Hyperthermia, commonly defined as the moderate hyperthermia ($41\text{ }^\circ\text{C} < T < 46\text{ }^\circ\text{C}$) is a treatment based on the generation of heat at tumor site to activate or initiate many intra- or extracellular degradation mechanisms that leads to death of cells.⁵⁷ However, the undifferentiated heating of both normal and malignant cells is a major concern.⁵⁸ PTT is a revolution in hyperthermia in which light is used to treat cancer with a spatiotemporally controlled and confined thermal damage.

Basically, light, which is the excitation source, and usually classified as ultraviolet (UV) light, visible light and near infrared (NIR) light, is necessary for PTT. Taking the advantage of good transmittance in biological tissues, NIR light, in the window between 700 and 1300 nm is intriguing. On the other hand, photothermal agent (PTA) is another requirement for highly absorbing light. Either natural chromophores in the tissue or externally added agents can be used as PTA, but the

latter ones are preferred because they have a much higher absorption, which can greatly reduce the amount of laser energy required. Externally added PTA mainly include dye molecules and NPs, among which, NPs are favored because of their flexible synthesis, easy surface modification, high stability with less photo-bleaching and low toxicity.

Gold-based materials, which include gold NPs (GNPs), gold nanorods (GNRs), gold shells (GSs), are the chief nanostructures that demonstrated in PTT. On account of the absorbance in NIR, they are usually with four to five orders of magnitude larger than those offered by photo-absorbing dyes, which is due to their surface plasmon resonance (SPR) oscillations.⁵⁹ Among these materials, GNPs are the earliest ones being studied. However, they absorb light strongly in the visible region.⁶⁰ Fortunately, SPR wavelength for GNPs is strongly dependent on their size, shape and the dielectric constant of the surrounding medium, which can redshift the absorption band to NIR region by increasing the size or aggregating/assembling NPs.⁶¹ By aggregating GNPs with a pH-sensitive polymer coating, Kim et al. shifts the absorption band from the near-red to the far-red region, and induced cell death under irradiation (Fig. 3a).⁶² When changing the spherical particle to non-spherical, the SPR spectrum would also be changed. Particularly for GNRs, the SPR spectrum splits into two bands, with a stronger long-wavelength band in the NIR region. Absorption spectrum of GNRs is very sensitive to the aspect ratio, i.e. with an increase in the aspect ratio, the SPR absorption peak significantly redshifts.⁵⁹ By changing the seed to gold salt ratio or the relative concentrations of the added impurities such as silver ions, El-Sayed and co-workers have demonstrated GNRs with different absorption band can be controlled synthesized (Fig. 3b).⁶³ The easy-controlling of GNRs makes it good candidates for PTT, which is widely applied both *in vitro* and *in vivo* in cancer therapy.^{64,65} Due to the spherical geometry, GSs can sustain large absorption cross sections in NIR, and their absorption light can be controlled by varying the shell thickness.⁶⁶ Moreover, the equivalently large diameter provides GSs in high absorption in NIR for PTT. Hwang et al. demonstrated that GSs can mediate the bimodal PTT and PDT (details in part 4.2) effects at ultra-low doses (28-150 mW/cm²) of NIR light excitation, and can kill the B16F0 melanoma tumors more efficiently than doxorubicin.⁶⁷ Additional advantages of GSs are their non-cytotoxicity and biocompatibility, leading to their current usage in clinical trials. The most commonly used GSs are in a silica-cored structure, such as gold shelled-silica,⁶⁸ gold-speckled silica NPs,⁶⁹ gold-shelled silica nanorattle.⁷⁰ However, most of their diameters are above 100 nm, which is harmful for long-circulation. Recently, Joshi et al. developed multilayered gold NPs (Au/SiO₂/Au) in the sub-100 nm size range. Due to strong coupling between the plasmons supported by the gold core and the gold shell, it exhibits enhanced accumulation in tumors, improved PTT effect and higher survival rate relative to a parallel treatment using single-layered GSs.⁷¹ Other gold-based materials, such as gold nanocubes,⁷² nanostars,^{73, 74} nanocages⁷⁵ and nanoheptapods⁷⁶ are also emerging as candidates for PTT.

Carbon-based materials, normally in forms of carbon nanotubes (CNTs) and graphene oxide (GO), are also important for PTT. CNTs, especially single-walled CNTs, can strongly absorb light in the NIR range (700-1400 nm), due to their unique physical, chemical and electrical properties. Moreover, as a unique quasi-one-dimensional material, CNTs could cross cellular membranes without eliciting cytotoxicity, being widely explored as agent for PTT.⁷⁷⁻⁸⁰ However, CNTs used usually consist of heterogeneous mixtures, with only a small subset of chirality nanotubes heated under a NIR laser. To overcome this problem, Dai et al. extracted the (6,5) chirality CNTs at a purity of ~80% and used an ultra-low dose of intravenous injection (~4 µg per mouse) to heat tumors to over 50 °C under 980 nm laser irradiation (Fig. 3c).⁸¹ GO, a single- or multi-layer of sp²-bonded carbon atoms, which is similar to CNTs, also possesses high NIR absorbance, being another important carbon-based material in PTT.^{82, 83} Except for the surface functionalization and size, redox state of GO is another important factor for PTT, with NIR absorbance being critically improved by reducing GO into reduced GO (rGO).^{84, 85} Khavan et al. found that rGO nanomesh exhibits about 22.4-fold higher NIR absorption at 808 nm than GO, which is assigned to partial restoration of the π network and the electronic conjugation among rGO sheets.⁸⁶ With the aid of rGO, cancer cell inhibition and tumor elimination can be achieved even at an ultralow laser power of 0.1 W/cm².^{86, 87} Recently, carbon shells are reported for their application in PTT. Dai's group found that graphitic carbon coated on FeCo can be heated under NIR irradiation, and it can suppress tumor growth accordingly.^{88, 89} We further investigated the heating phenomenon on novel Fe₅C₂ NPs, which possess a core/shell structure with a thin carbon coating. This shell makes its temperature to increase under an irradiation of 808 nm NIR light. By conjugating with an antibody (Fe₅C₂-Z_{HER2:342} NPs), it can selectively kill cancer cells, and completely eliminate tumor through intravenous injection together with NIR irradiation (Fig. 3d).⁷

Organic compounds such as indocyanine green dye⁹⁰ and polyaniline NPs,⁹¹ or micelles with dyes like IR825⁹² and IR780⁹³ are also involved in PTT, but they may suffer from limitations such as photo-bleaching or unsatisfactory photothermal conversion efficiency. Some other inorganic NPs with high NIR absorbance are developed in recent years, mainly including copper chalcogenide semiconductor NPs,⁹⁴⁻⁹⁶ tungsten chalcogenide nanowires or nanosheets,^{97, 98} showing great potential as agents for PTT.

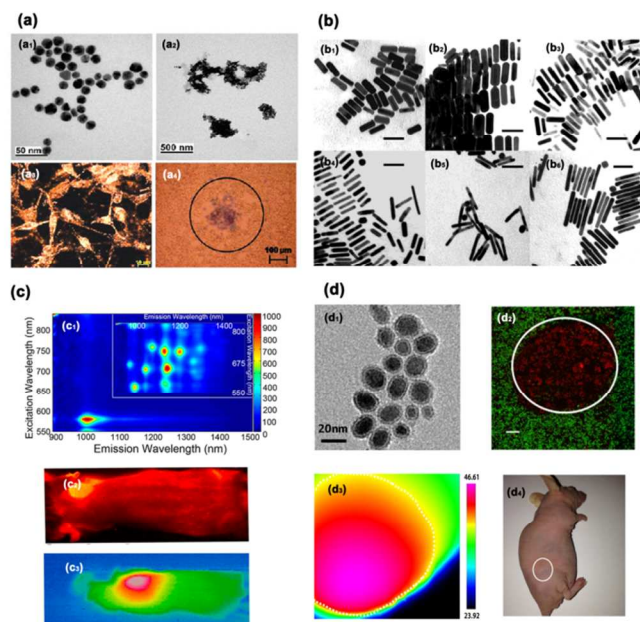


Fig. 3 (a) TEM image of (a₁) gold NPs and (a₂) their aggregation induced by acid environment. (a₃) Dark field microscope images of B16 F10 cells incubated with “smart” gold NPs, indicating efficient accumulation of “smart” gold NPs aggregates. (a₄) Photothermal destruction of HeLa cells incubated with “smart” gold NPs and irradiated with laser fluence rate of 10 W/cm².⁶² Reproduced with permission from ref. 62. Copyright 2009 American Chemical Society. (b) TEM images of gold NRs with plasmon band energies at (b₁) 700, (b₂) 760, (b₃) 790, (b₄) 880, (b₅) 1130, and (b₆) 1250 nm. The scale bar is 50 nm.⁶³ Reproduced with permission from ref. 63. Copyright 2003 American Chemical Society. (c) PTT by CNT. (c₁) Photoluminescence spectra of (6,5) chirality CNTs compared to as-synthesized HiPCO, confirming the absence of significant contamination from other chiralities. (c₂) NIR-II fluorescent imaging of mice 48 h post injection, showing clear CNTs accumulation in the 4T1 tumor. (c₃) Representative thermal images from tumor bearing mice 48 h after injection with (6,5) CNTs, and irradiation with 980 nm laser for 5 min.⁸¹ Reproduced with permission from ref. 81. Copyright 2013 American Chemical Society. (d) Fe₅C₂ NPs-based PTT. (d₁) TEM image of Fe₅C₂ NPs. (d₂) Fluorescence microscopy image of SK-OV-3 cells incubated with Fe₅C₂-Z_{HER2:342}, and irradiated with 808 nm laser. Necrotic or apoptotic cells were stained with PI and live cell were stained with Calcein-AM. (d₃) Infrared thermographic maps of tumor in mice treated with Fe₅C₂-Z_{HER2:342} NPs with laser. Fe₅C₂-Z_{HER2:342} NPs were injected through tail vein and the laser power density is 2 W/cm². (d₄) Photograph of mice from the group treating with Fe₅C₂-Z_{HER2:342} NPs and NIR irradiation.⁷ Reproduced with permission from ref. 7. Copyright 2014 WILEY-VCH Verlag GmbH & Co. KGaA, Weinheim.

4.2 Photodynamic therapy

PDT, a minimal invasive treatment of various diseases by using photosensitizers (PSs) along with the stimulation of light to generate ROS (usually singlet oxygen (¹O₂)), is emerging as an alternative to chemo- and radiotherapy.⁹⁹ However, most PSs are highly hydrophobic and require delivery systems. NPs are ideal carriers for PSs due to their large surface area, biocompatibility after modification, controlled PSs release and efficient uptake by cells. According to a review paper summarized by Konan et al., NPs for the delivery of PSs can be divided into passive NPs and active ones.¹⁰⁰ The former ones

are just carriers without interactions with light, while the latter ones can “react” with light by either directly being used as PSs to transfer energy to surrounding oxygen, or served as an energy donor to transduce energy to PSs. Quantum dots (QDs), upconversion NPs (UCNPs), and gold-based NPs are the mostly commonly studied active NPs in PDT.

Traditional passive NPs for PDT are usually some polymer-based materials, with the advantage of bio-degradable, high drug loading, and the possibility of controlling surface property, morphology, composition and the drug release. They are usually alternatives to liposomes, typically poly(lactic-co-glycolic acid (PLGA), polylactic acid (PLA) or their copolymers. By encapsulation PSs into NPs, therapeutic index can be improved compared with free PSs.^{101, 102} Photodynamic activity and the degradation rate of NPs are strongly affected by particle size, component and molar ratios of copolymer, and improved effect can be modulated accordingly.^{101, 103} These bio-degradable carrier, however, release PSs gradually, and the released PSs tend to accumulate in the skin and eye, resulting in phototoxic side effects lasting for at least a month.^{104, 105} Non-biodegradable ceramic-based NPs, normally silica, on the contrary, are alternatives owing to their stability. Possessing small size and exquisite controlling over size, shape and porosity, it holds advantages over biodegradable NPs.¹⁰⁶⁻¹¹⁰

QDs have been proposed as potential active vehicles for PDT due to their large absorbance cross-section and the tunable optical properties.^{111, 112} As a kind of PSs, QDs can accept electrons or hydrogen from other molecules, producing reactive intermediates that would induce irreversible damages and finally cell death (Fig. 4a I).¹¹²⁻¹¹⁶ However, because of the ultrafast relaxation of QDs compared with the slow energy transfer process with ¹O₂, as well as the relatively large hydrodynamic diameters of QDs, efficiency directly energy exchange with ¹O₂ is low.¹¹⁷ Reactive intermediates directly produced by QDs are usually hydrogen peroxide (H₂O₂), superoxide (O₂⁻), hydroxyl radicals (OH[•]), as well as reactive nitrogen species (RNS) like peroxyxynitrite (ONOO⁻).^{118, 119} There is another more general protocol of PDT based on QDs, which is associated to classical organic PSs by Förster Resonance Energy Transfer (FRET) with electron spin exchange, enabling the use of an excitation wavelength where the PSs alone does not absorb.¹²⁰ After combination with classical PSs, such as trifluoperazine,¹²¹ chlorin e6,^{111, 122} porphyrin,¹²³ and Foscan,¹²⁴ it can activate ¹O₂ generation by utilizing variable excitation wavelengths, and consequently kill cells effectively (Fig. 4a II). Recently, dopamine-QDs conjugate is reported as a new kind of PSs for PDT of cancers.¹²⁵ By accepting the electron from dopamine (DA) when excited by the visible light, the oxidized DA produces ¹O₂, with the yield comparable to that of sulfonated aluminum phthalocyanine.

One problem remained in PDT is that most currently used PSs are excited by visible or UV light, which exhibits poor tissue penetration, hampering applications in the treatment of large or internal tumors. NIR, in contrast, is a good choice for PDT, which not only can afford deeper penetration depths, but

also impose lower photo-toxicity on normal cells and tissues.¹²⁶ However, PDT efficiency reduced dramatically due to the low excitation of PSs when exposed to NIR. UCNP, usually lanthanide-doped NPs, can emit high energy photons under the excitation by NIR light, and are good candidates as energy donors. Loading PSs on UCNP with appropriate method is critical for PDT, as it would affect the efficiency of resonance energy transfer from UCNP to PSs. According to another review paper, there are three chief ways.¹²⁶ The mostly commonly used way is coating UCNP with a silica shell and PSs doped inside. This protocol can effectively kill cancer cells with high stability.¹²⁷⁻¹²⁹ Chu et al. designed UCNP that consist of NaYF₄ NPs co-doped with ytterbium (Yb³⁺) and erbium (Er³⁺) ions, followed by coating with a layer of PEI with zinc phthalocyanine attached onto the surface. Upon exposure to NIR light at 980 nm, the PSs absorb visible light, which is emitted by UCNP, and converts nearby molecular oxygen to

ROS, resulting in viral inactivation (Fig. 4b).¹²⁹ Non-covalent physical adsorption is another method by simply absorbing hydrophobic PSs such as chlorine 6 to UCNP through hydrophobic interaction.¹³⁰ This method offers effective resonance energy transfer due to the close binding between the UCNP and PSs. Covalent bonding strategy is the third protocol to link a PSs with UCNP, which can overcome the premature release of PSs.¹³¹

There are some other NPs being applied in PDT, such as plasmonic NPs and carbon-based materials, both of which are high in light absorbance at certain wavelength, being ideal energy transferors with the similar function of QDs.¹³² The plasmonic NPs mainly include GNPs, GNRs, GSs, gold nanocages and nanostars,¹³³⁻¹³⁸ and carbon-based materials usually contains carbon nanotube, graphene oxide and carbon quantum dots.¹³⁹⁻¹⁴²

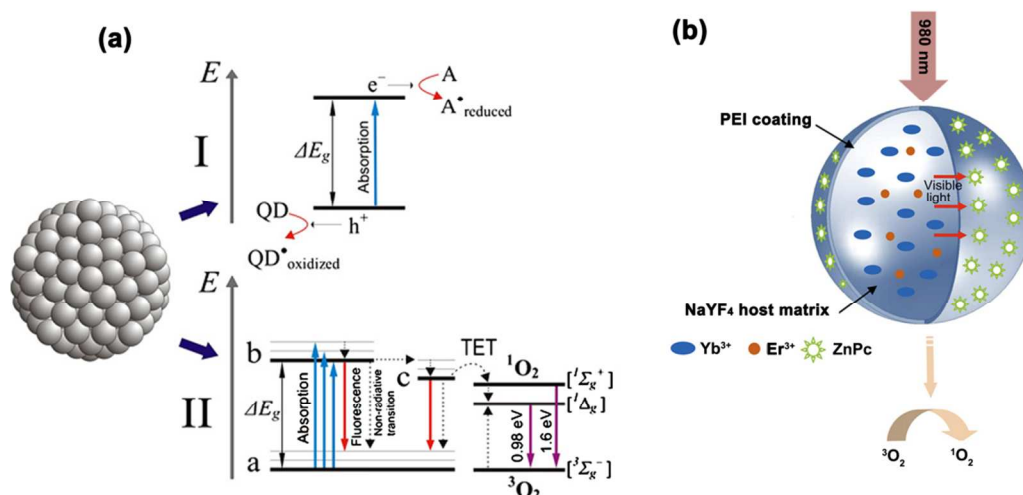


Fig. 4 (a) Schematic presentation of the most likely events occurring when a photon hits a quantum dot. (I) Charge transfer, where QD is a donor and A is an acceptor molecule; (II) Photosensitization, where QD is promoted from its ground state to a higher energy excited state and then to a “trap” state, from which by triplet energy transfer $^3\text{O}_2$ is promoted into a $^1\text{O}_2$.¹¹² Reproduced with permission from ref. 112. Copyright 2008 Elsevier. (b) Schematic drawing of UCNP structure and mechanism of action of UCNP-based PDT. The UCNP's core consists of NaYF₄ crystalline matrix doped with lanthanide ions of Yb³⁺ and Er³⁺.¹²⁹ Reproduced with permission from ref. 129. Copyright 2012 Elsevier.

4.3 Light-triggered delivery

Except for triggering drug release by chemical or bio-environment excitation, light is another attractive trigger which can remotely control the release spatially and temporally. Azo-containing azobenzene (AB), which can reversibly isomerized under irradiation, is the most studied molecular for light-responsive therapy. Under the irradiation with wavelength of 366 nm, *cis*-azo would be dominant, which will mostly revert back to *trans*-isomer when irradiated at wavelength > 420 nm.¹⁴³ Based on this intriguing concept, many systems are developed for the on-demand drug delivery. The early studies mainly focus on liposomes, micelles or polymers composed of the azo-based molecule, which encapsulate drugs inside, and can control the drug release according to the light wavelength.¹⁴⁴⁻¹⁴⁸ Later, the AB derivatives are developed as both impellers and gatekeepers. Due to the similarity of extinction coefficient for *cis*- and *trans*-AB at certain wavelength, when tethering on mesoporous silica NPs and irradiating at this wavelength, AB

moieties move back and forward, driving the drug molecules out of the silica.^{149, 150} According to this idea, Shi et al. developed a mesoporous silica-coated UCNP, which is further installed with AB groups and loaded with drug. Under the irradiation with wavelength of 980 nm, the reversible photo-isomerization by simultaneous UV and visible light emitted by the UCNP creates a continuous rotation-inversion movement for the back and forth wagging motion of the azo molecules, propelling the release of drug (Fig. 5a).¹⁵¹ Taking the advantage of the fact that *trans*-AB derivatives is in higher binding affinity with β -cyclodextrin (β -CD) compared with *cis*-isomer, light-induced delivery can also be realized. β -CD can seal drugs within carrier when conjugated with *trans*-AB. After irradiation, the isomerization of AB dissociated β -CD from carrier, opening the gates and releasing the drugs.¹⁵²⁻¹⁵⁴ For example, using the inclusion complex of *trans*-AB and CD as a photo-switchable crosslinker, Kros et al. constructed a dextran based photo-responsive hydrogel system. Upon the UV light irradiation, AB

moieties isomerize from *trans*- to *cis*-configurations, resulting in the dissociation of crosslinking points, and allowing the entrapped protein to migrate into the media (Fig. 5b).¹⁵⁴

Photo-sensitive bonds with cleavability under irradiation can also be used for light triggered delivery. *o*-nitrobenzyl ester is a typical bond, which can irreversibly cleavage the drug-particle bond or gatekeeper by transforming into *o*-nitrobenzaldehyde.^{155, 156} Coumarin is another group to be developed as “open-close door” for the on-demand delivery based on the dimerization/cleaving of the dimer, which is controlled by the light wavelength. Under irradiation with wavelength of 320-400 nm, the cycloaddition of a couple of coumarin moieties takes place to form a cyclobutane ring, while after irradiating by UV light ($\lambda=200-280$ nm), the coumarin photo-dimers can be cleaved and regenerate the coumarin moieties (Fig. 5c).^{157, 158} Taking this advantage, Shyu et al. functionalized mesoporous bioactive glasses (MBG) with coumarin, and operated the reversible gate dimerization.¹⁵⁸ Moreover, block copolymer contains either *o*-nitrobenzyl or coumarin moieties are proved to be two-photon absorbable,

which can be excited by NIR light, further extending their applications.¹⁵⁹

By embedding some PTT agents within temperature sensitive carriers, drug delivery can be controlled by light through heating.¹⁶⁰⁻¹⁶² The heat released also can dehybridize the double-stranded DNA, which would directly release the DNA segment for gene therapy or control the drug release by DNA. Qu et al. incorporates GNRs with a mesoporous silica framework which is surface-modified with aptamer DNA. Upon exposing to a laser beam, photo-energy is converted to heat, causing the dehybridization of duplex DNA and the release of G-quadruplex (Fig. 5d).¹⁶³ Meanwhile, the heat generated can also cleavage some temperature-sensitive linkages blocked on NPs, allowing the release of the entrapped guests.¹⁶³⁻¹⁶⁵ Together with PDT, photosensitization-induced oxidation is another photochemical mechanism to impart a change in a nanocarrier through light exposure.¹⁶⁶ ROS generated by PSs oxidizes plasmogenic lipids and DNA, thus causes disruption of bio-membranes, and provides spatial/temporal controlled endolysosomal escape of therapeutic molecules.¹⁶⁷⁻¹⁶⁹

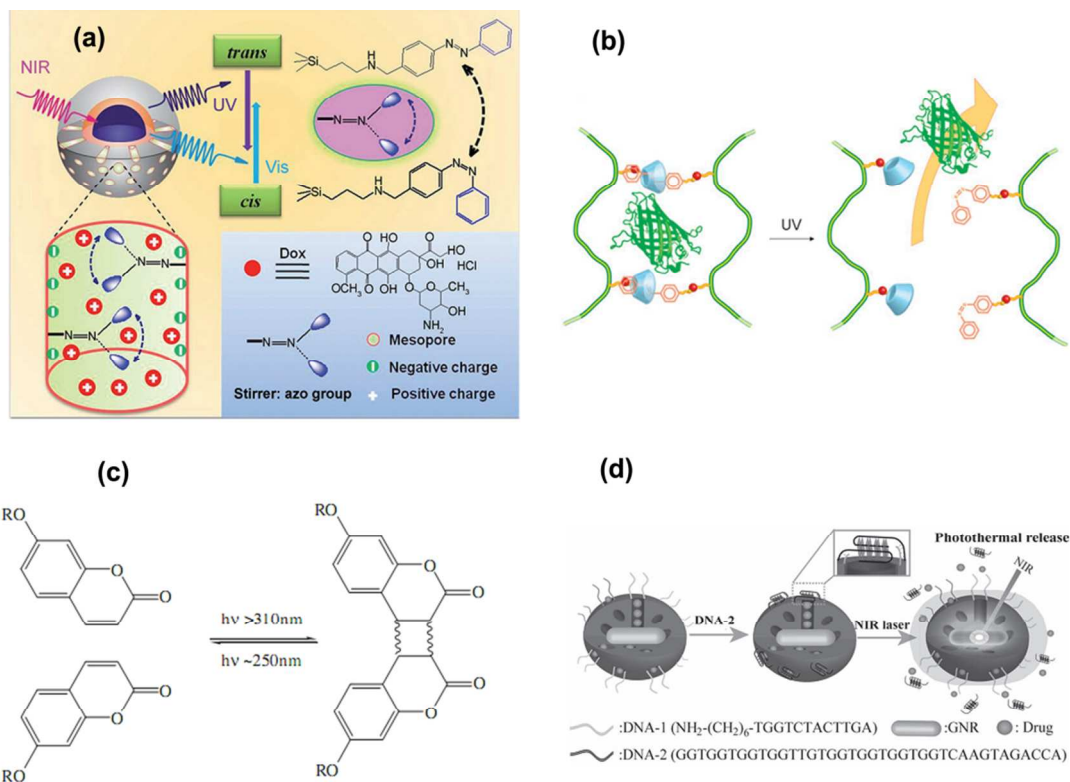


Fig. 5 (a) Schematic illustration of NIR light-triggered DOX releasing by making use of the upconversion property of UCNPs and *trans-cis* photoisomerization of azo molecules grafted in the mesopore network of a mesoporous silica layer.¹⁵¹ Reproduced with permission from ref. 151. Copyright 2013 WILEY-VCH Verlag GmbH & Co. KGaA, Weinheim. (b) Schematic representation of photo responsive protein release from the gel composed of *trans* AB modified dextran and CD modified dextran.¹⁵⁴ Reproduced with permission from ref. 154. Copyright 2010 Royal Society of Chemistry. (c) Schematic illustration of the photoreversible dimerization-cleavage reaction of coumarin derivative.¹⁵⁸ Reproduced with permission from ref. 158. Copyright 2010 Elsevier. (d) Schematic illustration for NIR light-triggered release of guest molecules from the pore of aptamer-covered nanovehicles.¹⁶³ Reproduced with permission from ref. 163. Copyright 2012 WILEY-VCH Verlag GmbH & Co. KGaA, Weinheim.

4.4 Imaging-guided therapy

To evaluate the bio-safety and therapeutic efficiency by visualizing the bio-distribution of the agent and monitoring the

treated sites, non-invasive guidance of therapeutic strategies with imaging is highly desired. Among the various imaging methods, optical imaging is one of the most widely adopted types, in both medicine and biological sciences.^{170, 171} Light responsive NPs, such as QDs, UCNPs and gold-based materials are the three crucial ones to be “lighted up” under irradiation.¹⁷²⁻¹⁷⁴ Basically, these materials would be fluorescent when excited by light from UV to NIR, which can be tuned by size control or doping. For instance, Chen et al. make full use of the fluorescence of QDs and the PTT by rGO, fabricating a QD-tagged rGO nanocomposite that combines the capability of cell/tumor bio-imaging with PTT after conjugation

with targeting/internalization ligands (Fig. 6a).¹⁷⁵ By further transforming heat into ultrasound, photoacoustic tomography (PAT), a recently developed imaging technique is usually combined with PTT for imaging-monitored therapy. Take Fe_3C_2 NPs for example, the PTT can be under the guidance of PAT (detailed in part 4.1). Moreover, the Fe_3C_2 NPs themselves are magnetic, which is suitable for T_2 -weighted magnetic resonance imaging (MRI) (discussed in part 5.5). The Hou’s group combined all of these interesting characteristics together, developing a targeted theranostic platform for MRI- and PAT-guided PTT (Fig. 6b).⁷

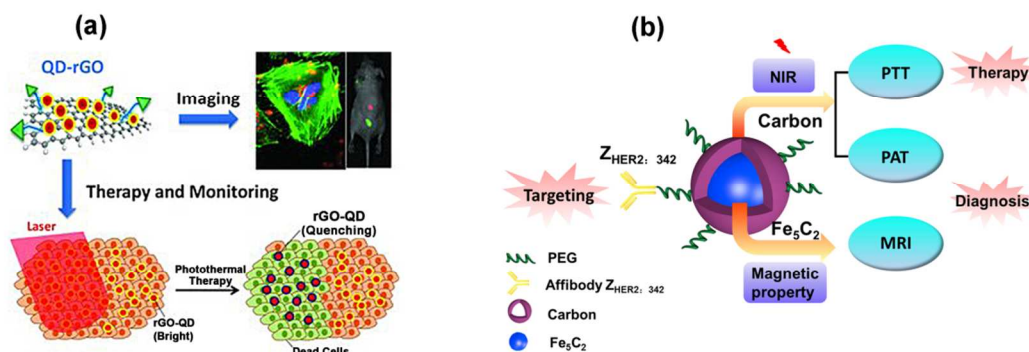


Fig. 6 (a) Schematic illustration of QDs-tagged rGO nanocomposites for bright fluorescence bioimaging and PTT.¹⁷⁵ Reproduced with permission from ref. 175. Copyright 2012 WILEY-VCH Verlag GmbH & Co. KGaA, Weinheim. (b) Schematic illustration for the designing of Fe_3C_2 NPs for targeted MRI- and PAT-guided PTT.⁷ Reproduced with permission from ref. 7. Copyright 2014 WILEY-VCH Verlag GmbH & Co. KGaA, Weinheim.

5. Magnetic field-triggered therapy

Certainly, light can well control the cancer therapy by optimizing its wavelength or intensity, however, treatment from large distances (>10 cm) cannot be achieved by such protocol.¹⁷⁶ Magnetic field, especially with the frequency below 400 Hz, on the contrary, is not significantly absorbed by tissue, permitting the remote-management without physical or chemical contact. Magnetic NPs (MNPs), with the ability of responding to magnetic field, can be applied in magnetic targeting for targeted drug and gene delivery, magnetically triggered drug/gene delivery, magnetic hyperthermia, magnetic controlled cell fate and MRI-guided therapy.¹⁷⁷

5.1 Magnetic Specific Targeting

Potential toxicity of NPs, especially the production of ROS, should be taken into consideration when they are applied.¹⁷⁸ Reducing the dose of NPs is one of the ways to minimize the potential toxicities. Apart from commonly used targeting techniques, including passive targeting and positive targeting, MNPs, with their ability to respond to an external magnetic field, have their own targeting method denoted as magnetic targeting. When exposed to an external magnetic field, MNPs can be magnetized, move under magnetic driving, and concentrate at a specific site.¹⁷⁹ Afterwards, NPs can be fixed at the desired local site due to the internalization by the endothelial cells at the targeted tissue (Fig. 7a).^{180, 181} By conjugation of drugs or gene on MNPs, this unique remotely

and noninvasively targeting process can be applied in actuation for drug delivery and gene translation.

So far, drug delivery by magnetic targeting has been applied in the targeting to various cancer cells, such as lung, prostate, brain, breast and liver cells. Similarly, benefiting from the magnetic force, for which can lead to either the enhancement of transfection efficiency or targeting to the specific site, both DNA and RNA have been transfected by MNPs (noted as magnetofection).¹⁷⁹ Compared with commercially available transfection agent, magnetofection can remarkably enhance the transfect efficiency in cell cultures, and improve the tolerance and the controlling of scenario *in vivo* as well.^{182, 183}

5.2 Magnetic-triggered drug/gene delivery

MNPs-based drug delivery, not only transports the drugs to a specific site, but also remotely controls drug release. Drugs can be attached to MNPs by conjugation on a heat sensitive linker¹⁸⁴ or through π - π interaction,¹⁸⁵ and in some situations, by co-embedding within thermal sensitive polymers.^{186, 187} Under an alternating magnetic field (AMF), MNPs can generate heat (details in part 5.3), which can improve the drug release due to the cracking of the linker or polymer (Fig. 7b).¹⁸⁸ Moreover, drugs can also be loaded into porous materials with MNPs as valves. The magnetic heat generation can build up pressure inside the porous NPs, removing the molecular valves and triggering the drug release (Fig. 7c).^{189, 190} Interestingly, compared to normal heating at the same temperature, drug release prompted by magnetic hyperthermia is much improved,

due to the synergistic effect of magnetic heating, magnetic disruption, and recrystallization.¹⁸⁸ Similarly, the overall efficiency of magnetofection can be further enhanced up to tenfold under oscillating magnetic arrays compared with magnetofection under static magnetic fields. Dobson et al.

attributed it to the association of magnetic vectors with membranes, and the transmission of mechanical forces from the lateral movement of the magnetic field to cellular membranes (Fig. 7d).^{191, 192}

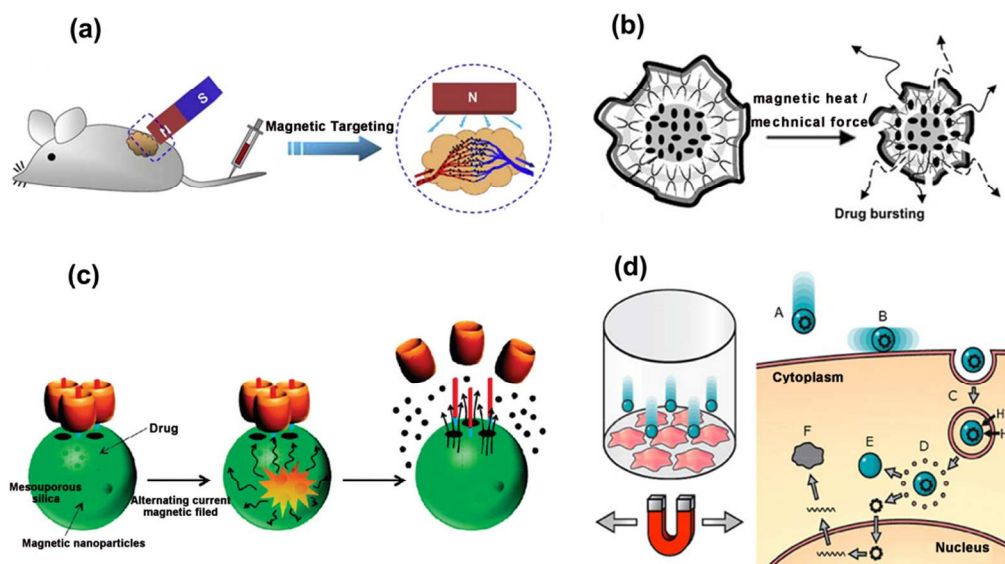


Fig. 7 (a) A schematic illustration shows the concept of magnetically targeting.¹⁸¹ Reproduced with permission from ref. 181. Copyright 2012 Elsevier. (b,c) Schematics of remotely controlling of drug release through (b) shrinkage or deformation of polymers and (c) molecular valves.^{188, 190} Reproduced with permission from ref. 188. Copyright 2009 WILEY-VCH Verlag GmbH & Co. KGaA, Weinheim. Reproduced with permission from ref. 190. Copyright 2011, American Chemical Society. (d) Principle of oscillating nanomagnetic transfection. Plasmid DNA or siRNA is attached to MNPs and incubated with cells in culture (left). An oscillating magnet array below the surface of the cell culture plate (A) pulls the particles into contact with the cell membrane and (B) drags the particles from side to side across the cells, (C) then mechanically stimulating endocytosis. Once the particle/DNA complex is endocytosed, (D) proton sponge effects rupture the endosome, (E) releasing the DNA, which (F) then transcribes the target protein.¹⁹¹ Reproduced with permission from ref. 191. Copyright 2012 Indian Academy of Sciences.

5.3 Magnetic hyperthermia

Under an AMF, the unique property of MNPs allows them go through a hysteretic process or relaxation behavior to generate heat, which is named as magnetic hyperthermia. Compared with PTT, magnetic hyperthermia can target when residing deep inside the biological system without penetration depth problem, and the magnetic field causes no adverse effect on biological tissues, which is distinctively beneficial for noninvasive *in vivo* applications.^{193,194}

By using the thermal energy generated by MNPs, cancer can be conquered by launching cell death or prompting the immune system directly. With the stimulation of a “initiator” cysteinyl aspartate-specific protease (caspase), apoptosis, a programmed cells death way can be induced by magnetic hyperthermia, which can be identified by morphological changes, including formation of membrane blebbing, cell rounding, and detach of actin.^{195, 196} Both caspase 3 and 7, and even TNF- α gene expression can be induced by MNPs in a magnetically modulated cancer hyperthermia way, all of which showed an excellent antitumor efficacy without severe toxicity (Fig. 8a).^{197, 198} Interestingly, apoptosis induced by this method is more severe than that by hot water, although the mechanisms are still unknown.¹⁹⁹ Cell necrosis, a cell death triggered by directly destroying the cellular structure, including loss of

membrane structure and shrink of the cells, can also be realized by magnetic hyperthermia (Fig. 8b).^{200, 201} After being engulfed into the endosome and exposed to AMF, MNPs can disrupt the endosomal membrane by heat, and the released endosomal content can damage the cell membrane.²⁰¹ Even when MNPs are just dropped on the membrane without being engulfed into cells, heat generated can also disturb the membrane structure directly to induce cell necrosis.²⁰² Magnetic hyperthermia is also able to activate an immune response by heat shock to reduce both primary tumor and metastatic lesions.²⁰³ It is astonishing that when only one tumor was subjected to magnetic hyperthermia, both tumors at each femur in T-9 rat disappeared after the treatment, due to the activation of natural killer cell when temperature rise to 42 °C in the presence of heat shock proteins.²⁰⁴ This hyperthermia triggering immunotherapy shows a great promise for rejecting tumors, especially metastasis tumor, which is now a challenge to cure.

To induce higher temperature by MNPs with fewer dose added, factors to influence the heating power are widely studied, which mainly including the AMF applied and the structures, morphology and size of MNPs.^{197, 202, 205} Briefly, the heating power is proportional to the amplitude and frequency of AMF as well as magnetization of MNPs, and inversely proportional to the size distribution of MNPs.^{206, 207} Additionally, properly

modifying of MNPs can also improve the heating power. Pawar et al found that hyperthermia effect of Fe_3O_4 NPs can be enhanced dramatically after functionalization with chitosan/glutaraldehyde due to the improved water solubility.²⁰⁸ Based on this phenomenon, we developed an aqueous solution of Fe_3O_4 NPs with a ferrofluidic behavior through the ligand exchange protocol with protocatechuic acid. This solution is highly stable in water, and can be heated from 36 °C to 46 °C within 5 min with the concentration of only 1 mg/mL (Fig. 8c).²⁰⁹

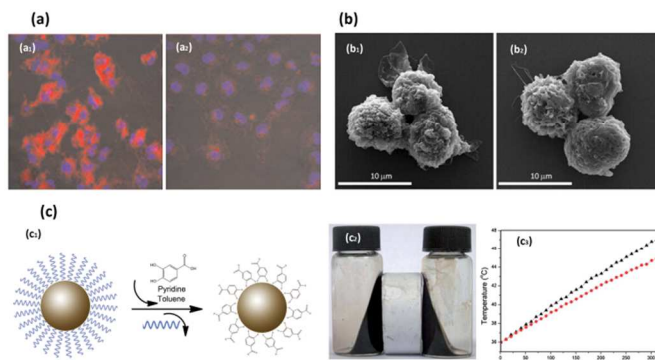


Fig. 8 (a) Cellular apoptotic activity of chitosan oligosaccharide-stabilized ferrimagnetic iron oxide nanocubes (Chito-FIONs) treated A549 cells (a₁) inside and (a₂) outside the area exposed to a magnet and subsequent application of an AMF. Cellular apoptotic activity was detected by using a red fluorogenic substrate for caspases 3 and 7 (red), and cell nuclei were stained with DAPI.¹⁹⁷ Reproduced with permission from ref. 197. Copyright 2012, American Chemical Society. (b) SEM images of dendritic cells loaded with MNPs (b₁) before and (b₂) after the application of the AMF. A partial collapse of the membrane structures can be observed after exposure to AMF.²⁰¹ Reproduced with permission from ref. 201. Copyright 2012 Royal Society of Chemistry. (c₁) Schematic illustration of the rapid ligand exchange process of Fe_3O_4 NPs. (c₂) Photographs of the ferrofluidic behavior of as synthesized Fe_3O_4 NPs in hexane (left) and in water after modification

(right). Temperature profile during the hyperthermia experiment of 12 nm Fe_3O_4 NPs (red) and 25 nm Fe_3O_4 NPs (black).²⁰⁹ Reproduced with permission from ref. 209. Copyright 2013 Royal Society of Chemistry.

5.4 Magnetic Switches for Cell Fate Control

Under exposure to an external magnetic fields, some cell signaling pathways such as F-actin arrangement, cell alignment, intracellular ion fluctuations and mitochondria activation may be changed.^{210, 211} But these activations only need force in the order of 10^{-15} - 10^{-12} N (fN-pN), while some other activations, including antibody-antigen interaction, require a stronger force in the 10^{-9} N order (nN), and cannot be excited by magnetic field only.^{212, 213} By introducing MNPs, the influence of magnetic field to cells will be enlarged dramatically due to their specific response to magnetic field. After conjugating with antibody or some ligands on MNPs, receptors of interest can be controlled precisely by generating mechanical stimulations of magnetic drag, rotation or twisting through the interaction of MNPs and cells, and finally influence cell growth, differentiation or even death.^{214, 215} Cheon et al. induced strong attractive forces between neighboring NPs by static magnetic field with Zn^{2+} -doped ferrite MNPs, which prompted the clustering of specific protein after interacting with certain receptor, triggering cell apoptosis signaling pathways without damaging the cell membranes (Fig. 9a).^{216, 217} AMF can also activate MNPs except for the magnetic hyperthermia. Gao et al. designed a magnetolytic therapy by using MNPs with their magnetic and non-magnetic part separately. Due to the asymmetry in spatial distribution of magnetic component, NPs can rotate under a spinning magnetic field after attaching on cells, killing the tumor cells owing to the compromised integrity of the cell membrane, and then, promoting cell apoptosis (Fig. 9b).²¹⁸

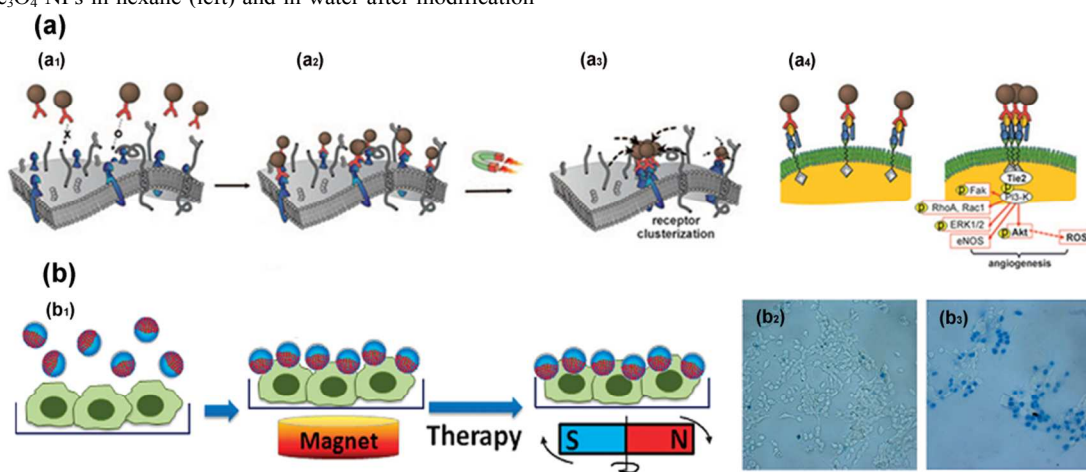


Fig. 9 (a) Targeting and magnetic manipulation of Ab-Zn-MNPs. (a_{1,2}) Ab-Zn-MNPs selectively bind to the specific cell-surface Tie2 receptors. (a₃) In the presence of an external magnetic field, the Ab-Zn-MNPs are magnetized to form nanoparticle aggregates, and induce the clustering of receptors to trigger intracellular signaling. (a₄) Tie2 receptor-bound NPs before and after application of the magnetic field.²¹⁶ Reproduced with permission from ref. 216. Copyright 2010 WILEY-VCH Verlag GmbH & Co. KGaA, Weinheim. (b) magnetolytic therapy. (b₁) Schematic illustration of the experimental conditions and magnetolytic therapy. (b_{2,3}) Magnetolytic therapy on tumor cells: (b₂) control group without NPs and magnetic field off. (b₃) group with NPs and magnetic field on. Dead cells appear blue due to Trypan blue staining.²¹⁸ Reproduced with permission from ref. 218. Copyright 2010 American Chemical Society.

ARTICLE

5.5 MRI-monitoring cancer therapy

Apart from the aforementioned optical imaging, there is another clinically used imaging method for cancer diagnosis called MRI, which has high resolution and deep tissue penetration. MNPs with unique magnetic property are able to improve the signal to noise ratio in MRI, and have been widely applied as MRI contrast agents. Together with excellent therapeutic effects realized by any means discussed previously, MNPs can be applied in the MRI-guided cancer therapy.^{219, 220}

Generally, there are two modes in MRI, which are termed as T_1 -weighted MRI and T_2 -weighted MRI. The former one is clinically favored as they provide positive signal, which is bright in images. Paramagnetic gadolinium- and manganese-based NPs, with seven and five unpaired electrons respectively, are the most widely used contrast agents for T_1 -weighted MRI. Taking the advantage of the pH-sensitivity of HMP NPs, which would release Mn^{2+} under low pH value (detailed discussed in part 2), the pH-sensitive drug delivery can be realized under the guidance of MRI (Fig. 1c). By further loading siRNA on low molecular weight amphiphilic Alkyl-PEI2k modified MnO NPs, we can effectively bind and deliver firefly luciferase (fluc) siRNA into 4T1-fluc cells, and tracked this process by T_1 -weighted MRI (Fig. 10a).²²¹ For better accuracy in delineating

the tumor, multi-modality imaging-guided therapy is required. Recently, Gambhir et al. reported a MRI-PAT-Raman imaging triple-modality imaging, which was used to detect brain tumor margins in mice, showed the three modalities are all in a sensitivity of at least picomolar order.²²² However, due to the possible toxicity issues of Mn^{2+} and Gd^{3+} , alternatives for these materials are pursued. Fe_3O_4 is a good candidate due to the possession of paramagnetic Fe^{3+} as well as their high saturation magnetization for T_2 -weighted MRI. Recently, some work have confirmed the feasibility of T_1/T_2 dual-modality contrast agents based on Fe_3O_4 NPs only.²²³ By exploiting this intriguing property, we developed Fe_3O_4 NPs into a dual mode MRI with a properly modification (detailed description in part 5.3). After injecting into a rabbit through its ear vein, the T_1 -weighted image showed a significant contrast enhancement of heart and blood vessels, while the T_2 -weighted image displayed a completely darkening in liver within 3 min (Fig. 10b), which would be hopeful for MRI-guided magnetic hyperthermia.²⁰⁹ In addition, this promising technique can also monitor changes of tumor size and its microenvironment, as well as in the situation for supervising atherosclerosis.^{224, 225} It opens a new era for the efficient management of therapy which is “visible” for the therapeutic mechanism and effect.

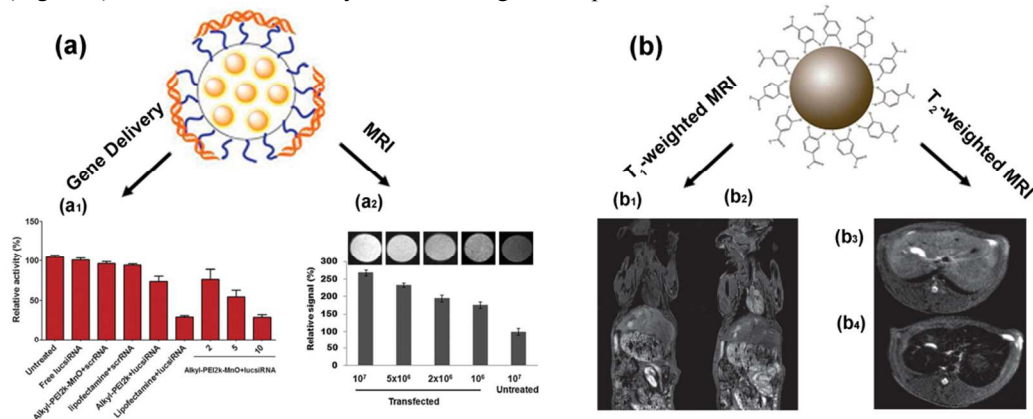


Fig. 10 (a) T_1 -weighted MRI-tracked gene delivery. (a₁) Bioluminescence imaging signal intensity of the transfected 4T1-fluc cells after being exposed to Alkyl-PEI2k-MnO/siRNA complexes at different N/P ratios. (a₂) Relative T_1 signal intensity at different cell amounts after Alkyl-PEI2k-MnO/siRNA transfection.²²¹ Reproduced with permission from ref. 221. Copyright 2011 Royal Society of Chemistry. (b) Developing Fe_3O_4 as dual-mode MRI contrast agent for diagnostics. (b₁, b₂) T_1 -weighted images of rabbit (b₁) before and (b₂) after injection of 12 nm Fe_3O_4 NPs. (b₃, b₄) T_2 -weighted images of rabbit (b₃) before and (b₄) 24 h after injection of 12 nm Fe_3O_4 NPs.²⁰⁹ Reproduced with permission from ref. 209. Copyright 2013 Royal Society of Chemistry.

6. Conclusions and perspectives

Tremendous efforts have been made during the last few decades to overcome cancer with low side effects. Stimuli-responsive NPs, which are commonly developed as drug/gene carrier for an on-demand releasing, have a great potential for

the individual therapy. When exposed to cancer internal environment or undergoing an external stimulus, NPs change their structures or morphologies to release the loaded drug/gene. But when it is unnecessary, there is no leakage to normal tissues. Sometimes, NPs themselves are developed as potential “drugs”, which can release signals, such as heat, poison ions,

and mechanical force to kill cancer cells only when they received certain stimuli. To reach these goals, NPs for controlled therapy should possess the following features: (1) non-toxicity; (2) the ability to target cancer tissues and enhance the cancerous cellular uptake; (3) the fast responsive ability to a stimulus; (4) good stability and minimal drug loss during circulation when used as a carrier.

Challenges still remain despite considerable achievements in stimulus-responsive NPs-based cancer therapy. Most systems discussed above respond to only a single type of signal, which could only interact with a fraction of tumor cells overexpressing the signal, causing low overall therapeutic efficacy.⁴⁶ In addition, each therapeutic modality has its own limitations. For instance, internal-environment-responsive therapies, such as pH- and light- triggered ones are with low flexibility compared with external-stimuli controlled modality, while light-related therapy is limited by shallow penetration, and magnetic NPs-based therapies need high concentrations of NPs to work. Moreover, biological systems sometimes need two different stimulus signals to trigger enzymatic functions.²²⁶ To better apply NPs in the “intelligent” therapy, it often require NPs being sensitive to multiple environmental changes rather than a single signal. Recently, pH- and redox-,²²⁷ glucose- and pH-,²²⁸ magnetic- and pH-²²⁹ dual-responsive NPs, and even reduction-, temperature- and enzyme²³⁰ tri-stimuli active NPs have been reported. However, they are just emerging, and need further explorations. Moreover, NPs which are used nowadays, especially the inorganic NPs, are non-biodegradable and sometimes harmful when exposed to biological systems for a long period time. For example, iron-containing NPs may release ferrous (Fe^{2+}) and/or ferric (Fe^{3+}) ions, and the acceptance and donation of electrons between these two ions may cause an imbalance in body homeostasis and lead to aberrant cellular responses, such as DNA damage, oxidative stress, and inflammatory processes. In the future, we expect to reap the benefits of combined stimulus-sensitive NPs with easy excretion and good biocompatibility for effective cancer therapy.

Acknowledgements

This work was partially supported by National Natural Science Foundation of China (NSFC) (nos. 51125001 and 51172005), the Research Fellowship for International Young Scientists of the National Natural Science Foundation of China (grant no. 51250110078), the National Basic Research Program of China (no. 2010CB934601), the Doctoral Program (no. 20090001120010), the Natural Science Foundation of Beijing (2122022), and PKU COE-Health Science Center Seed Fund.

Notes and references

- ^a Department of Materials Science and Engineering, College of Engineering, Peking University, Beijing 100871, China. E-mail: houl@pku.edu.cn
- X. He, J. Li, S. An and C. Jiang, *Ther. Deliv.*, 2013, **4**, 1499-1510.
 - Y. Li, G. H. Gao and D. S. Lee, *Adv. Healthc. Mater.*, 2013, **2**, 388-417.
 - D. J. Slamon, G. M. Clark, S. G. Wong, W. J. Levin, A. Ullrich and W. L. McGuire, *Science*, 1987, **235**, 177-182.
 - J. Yu, R. Hao, F. Sheng, L. Xu, G. Li and Y. Hou, *Nano Res.*, 2012, **5**, 679-694.
 - J. Y. Yhee, S. J. Lee, S. Lee, S. Song, H. S. Min, S.-W. Kang, S. Son, S. Y. Jeong, I. C. Kwon, S. H. Kim and K. Kim, *Bioconjugate Chem.*, 2013, **24**, 1850-1860.
 - F. Danhier, A. L. Breton and V. Préat, *Mol. Pharm.*, 2012, **9**, 2961-2973.
 - J. Yu, C. Yang, J. Li, Y. Ding, L. Zhang, M. Z. Yousaf, J. Lin, R. Pang, L. Wei, L. Xu, F. Sheng, C. Li, G. Li, L. Zhao and Y. Hou, *Adv. Mater.*, 2014, **26**, 4114-4120.
 - V. Shirshahi, F. Shamsipour, A. Zarnani, J. Verdi and R. Saber, *Cancer Nano*, 2013, **4**, 27-37.
 - L. Han, H. J. Ma, Y. B. Guo, Y. Y. Kuang, X. He and C. Jiang, *Adv. Healthc. Mater.*, 2013, **2**, 1435-1439.
 - H. Cho, J. Bae, V. K. Garripelli, J. M. Anderson, H.-W. Jun and S. Jo, *Chem. Commun.*, 2012, **48**, 6043-6045.
 - J. Zhang, Z. F. Yuan, Y. Wang, W. H. Chen, G. F. Luo, S. X. Cheng, R. X. Zhuo and X. Z. Zhang, *J. Am. Chem. Soc.*, 2013, **135**, 5068-5073.
 - S. E. Lee, G. L. Liu, F. Kim and L. P. Lee, *Nano Lett.*, 2009, **9**, 562-570.
 - C. Liu, J. Guo, W. Yang, J. Hu, C. Wang and S. Fu, *J. Mater. Chem.*, 2009, **19**, 4764-4770.
 - T. H. Yu, S. G. Li, J. Zhao and T. J. Mason, *Technol. Cancer Res. Treat.*, 2006, **5**, 51-60.
 - J. Xie and S. Jon, *Theranostics*, 2012, **2**, 122-124.
 - R. Hao, R. Xing, Z. Xu, Y. Hou, S. Gao and S. Sun, *Adv. Mater.*, 2010, **22**, 2729-2742.
 - Y. Wang, K. Zhou, G. Huang, C. Hensley, X. Huang, X. Ma, T. Zhao, B. D. Sumer, R. J. DeBerardinis and J. Gao, *Nat. Mater.*, 2014, **13**, 204-212.
 - E. Aznar, M. D. Marcos, R. Martínez-Mañez, F. Sancenón, J. Soto, P. Amorós and C. Guillem, *J. Am. Chem. Soc.*, 2009, **131**, 6833-6843.
 - R. Liu, Y. Zhang, X. Zhao, A. Agarwal, L. J. Mueller and P. Feng, *J. Am. Chem. Soc.*, 2010, **132**, 1500-1501.
 - Y. Bae, N. Nishiyama and K. Kataoka, *Bioconjugate Chem.*, 2007, **18**, 1131-1139.
 - S. Jung, J. Nam, S. Hwang, J. Park, J. Hur, K. Im, N. Park and S. Kim, *Anal. Chem.*, 2013, **85**, 7674-7681.
 - Q. Gan, X. Lu, W. Dong, Y. Yuan, J. Qian, Y. Li, J. Shi and C. Liu, *J. Mater. Chem.*, 2012, **22**, 15960-15968.
 - B. Wang, C. Xu, J. Xie, Z. Yang and S. Sun, *J. Am. Chem. Soc.*, 2008, **130**, 14436-14437.
 - C. Gao, H. Zheng, L. Xing, M. Shu and S. Che, *Chem. Mater.*, 2010, **22**, 5437-5444.
 - C. Li, L. Xing and S. Che, *Dalton Trans.*, 2012, **41**, 3714-3719.
 - C.-H. Lee, L.-W. Lo, C.-Y. Mou and C.-S. Yang, *Adv. Funct. Mater.*, 2008, **18**, 3283-3292.
 - S. Li, J. Zheng, D. Chen, Y. Wu, W. Zhang, F. Zheng, J. Cao, H. Ma and Y. Liu, *Nanoscale*, 2013, **5**, 11718-11724.

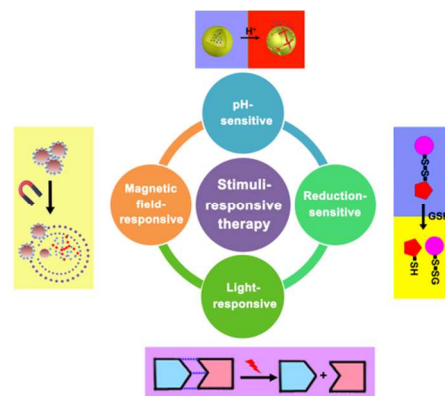
28. V. N. Phan, E.-K. Lim, T. Kim, M. Kim, Y. Choi, B. Kim, M. Lee, A. Oh, J. Jin, Y. Chae, H. Baik, J.-S. Suh, S. Haam, Y.-M. Huh and K. Lee, *Adv. Mater.*, 2013, **25**, 3202-3208.
29. R. J. Xing, A. A. Bhirde, S. J. Wang, X. L. Sun, G. Liu, Y. L. Hou and X. Y. Chen, *Nano Res.*, 2013, **6**, 1-9.
30. Y. Chen, Q. Yin, X. F. Ji, S. J. Zhang, H. R. Chen, Y. Y. Zheng, Y. Sun, H. Y. Qu, Z. Wang, Y. P. Li, X. Wang, K. Zhang, L. L. Zhang and J. L. Shi, *Biomaterials*, 2012, **33**, 7126-7137.
31. M. F. Bennewitz, T. L. Lobo, M. K. Nkansah, G. Ulas, G. W. Brudvig and E. M. Shapiro, *ACS Nano*, 2011, **5**, 3438-3446.
32. K. Cheng, S. Peng, C. Xu and S. Sun, *J. Am. Chem. Soc.*, 2009, **131**, 10637-10644.
33. F. Muhammad, M. Guo, W. Qi, F. Sun, A. Wang, Y. Guo and G. Zhu, *J. Am. Chem. Soc.*, 2011, **133**, 8778-8781.
34. X. Ying, C. Shan, K. Jiang, Z. Chen and Y. Du, *RSC Adv.*, 2014, **4**, 10841-10844.
35. C. J. Xu, Z. L. Yuan, N. Kohler, J. M. Kim, M. A. Chung and S. H. Sun, *J. Am. Chem. Soc.*, 2009, **131**, 15346-15351.
36. C.-J. Ke, T.-Y. Su, H.-L. Chen, H.-L. Liu, W.-L. Chiang, P.-C. Chu, Y. Xia and H.-W. Sung, *Angew. Chem. Int. Ed.*, 2011, **50**, 8086-8089.
37. J. J. Khandare, A. Jalota-Badhar, N. Taneja, R. R. Mascarenhas, K. Vadodaria, K. R. Zope and S. S. Banerjee, *Part. Part. Syst. Charact.*, 2013, **30**, 494-500.
38. P. Kuppusamy, H. Q. Li, G. Ilangovan, A. J. Cardounel, J. L. Zweier, K. Yamada, M. C. Krishna and J. B. Mitchell, *Cancer Res.*, 2002, **62**, 307-312.
39. R. Cheng, F. Feng, F. Meng, C. Deng, J. Feijen and Z. Zhong, *J. Control. Release*, 2011, **152**, 2-12.
40. M. Huo, J. Yuan, L. Tao and Y. Wei, *Polym. Chem.*, 2014, **5**, 1519-1528.
41. M. H. Lee, Z. Yang, C. W. Lim, Y. H. Lee, S. Dongbang, C. Kang and J. S. Kim, *Chem. Rev.*, 2013, **113**, 5071-5109.
42. W. A. Henne, D. D. Doorneweerd, A. R. Hilgenbrink, S. A. Kularatne and P. S. Low, *Bioorg. Med. Chem. Lett.*, 2006, **16**, 5350-5355.
43. S. Y. Chen, X. R. Zhao, J. Y. Chen, J. Chen, L. Kuznetsova, S. S. Wong and I. Ojima, *Bioconjugate Chem.*, 2010, **21**, 979-987.
44. S. Santra, C. Kaittanis, O. J. Santiesteban and J. M. Perez, *J. Am. Chem. Soc.*, 2011, **133**, 16680-16688.
45. M. Ma, H. R. Chen, Y. Chen, X. Wang, F. Chen, X. Z. Cui and J. L. Shi, *Biomaterials*, 2012, **33**, 989-998.
46. J. Wang, X. Sun, W. Mao, W. Sun, J. Tang, M. Sui, Y. Shen and Z. Gu, *Adv. Mater.*, 2013, **25**, 3670-3676.
47. Z. Zhou, Y. Shen, J. Tang, M. Fan, E. A. Van Kirk, W. J. Murdoch and M. Radosz, *Adv. Funct. Mater.*, 2009, **19**, 3580-3589.
48. P. Liu, B. Shi, C. Yue, G. Gao, P. Li, H. Yi, M. Li, B. Wang, Y. Ma and L. Cai, *Polym. Chem.*, 2013, **4**, 5793-5799.
49. P. Liu, C. Yue, Z. Sheng, G. Gao, M. Li, H. Yi, C. Zheng, B. Wang and L. Cai, *Polym. Chem.*, 2014, **5**, 874-881.
50. S. Cajot, N. Lautram, C. Passirani and C. Jerome, *J. Control. Release*, 2011, **152**, 30-36.
51. Y.-C. Wang, F. Wang, T.-M. Sun and J. Wang, *Bioconjugate Chem.*, 2011, **22**, 1939-1945.
52. S. Yu, J. Ding, C. He, Y. Cao, W. Xu and X. Chen, *Adv. Healthc. Mater.*, 2014, **3**, 752-760.
53. H. Kim, S. Kim, C. Park, H. Lee, H. J. Park and C. Kim, *Adv. Mater.*, 2010, **22**, 4280-4283.
54. Z. Luo, K. Cai, Y. Hu, L. Zhao, P. Liu, L. Duan and W. Yang, *Angew. Chem. Int. Ed.*, 2011, **50**, 640-643.
55. N. Ma, Y. Li, H. Xu, Z. Wang and X. Zhang, *J. Am. Chem. Soc.*, 2009, **132**, 442-443.
56. R. Cheng, F. Meng, C. Deng, H.-A. Klok and Z. Zhong, *Biomaterials*, 2013, **34**, 3647-3657.
57. C. S. S. R. Kumar and F. Mohammad, *Adv. Drug Deliv. Rev.*, 2011, **63**, 789-808.
58. S. Bhattacharyya, R. Kudgus, R. Bhattacharya and P. Mukherjee, *Pharm. Res.*, 2011, **28**, 237-259.
59. X. Huang, P. Jain, I. El-Sayed and M. El-Sayed, *Lasers Med. Sci.*, 2008, **23**, 217-228.
60. S. Link and M. A. El-Sayed, *J. Phys. Chem. B*, 1999, **103**, 4212-4217.
61. P. K. Jain, K. S. Lee, I. H. El-Sayed and M. A. El-Sayed, *J. Phys. Chem. B*, 2006, **110**, 7238-7248.
62. J. Nam, N. Won, H. Jin, H. Chung and S. Kim, *J. Am. Chem. Soc.*, 2009, **131**, 13639-13645.
63. B. Nikoobakht and M. A. El-Sayed, *Chem. Mater.*, 2003, **15**, 1957-1962.
64. M. A. Mackey, M. R. K. Ali, L. A. Austin, R. D. Near and M. A. El-Sayed, *J. Phys. Chem. B*, 2014, **118**, 1319-1326.
66. W. I. Choi, J.-Y. Kim, C. Kang, C. C. Byeon, Y. H. Kim and G. Tee, *ACS Nano*, 2011, **5**, 1995-2003.
66. E. Prodan, C. Radloff, N. J. Halas and P. Nordlander, *Science*, 2003, **302**, 419-422.
67. R. Vankayala, C.-C. Lin, P. Kalluru, C.-S. Chiang and K. C. Hwang, *Biomaterials*, 2014, **35**, 5527-5538.
68. S.-Y. Liu, Z.-S. Liang, F. Gao, S.-F. Luo and G.-Q. Lu, *J. Mater. Sci.-Mater. Med.*, 2010, **21**, 665-674.
69. P. Sharma, S. C. Brown, A. Singh, N. Iwakuma, G. Pyrgiotakis, V. Krishna, J. A. Knapik, K. Barr, B. M. Moudgil and S. R. Grobmyer, *J. Mater. Chem.*, 2010, **20**, 5182-5185.
70. H. Y. Liu, D. Chen, L. L. Li, T. L. Liu, L. F. Tan, X. L. Wu and F. Q. Tang, *Angew. Chem. Int. Ed.*, 2011, **50**, 891-895.
71. C. Ayala-Orozco, C. Urban, M. W. Knight, A. S. Urban, O. Neumann, S. W. Bishnoi, S. Mukherjee, A. M. Goodman, H. Charron, T. Mitchell, M. Shea, R. Roy, S. Nanda, R. Schiff, N. J. Halas and A. Joshi, *ACS Nano*, 2014, **8**, 6372-6381.
72. X. Wu, T. Ming, X. Wang, P. Wang, J. Wang and J. Chen, *ACS Nano*, 2009, **4**, 113-120.
73. S. Wang, P. Huang, L. Nie, R. Xing, D. Liu, Z. Wang, J. Lin, S. Chen, G. Niu, G. Lu and X. Chen, *Adv. Mater.*, 2013, **25**, 3055-3061.
74. H. Yuan, A. M. Fales and T. Vo-Dinh, *J. Am. Chem. Soc.*, 2012, **134**, 11358-11361.
75. C. Jingyi, C. Glaus, R. Laforest, Z. Qiang, Y. Miaoxian, M. Gidding, M. J. Welch and X. Younan, *Small*, 2010, **6**, 811-817.
76. Y. Wang, K. C. L. Black, H. Luehmann, W. Li, Y. Zhang, X. Cai, D. Wan, S.-Y. Liu, M. Li, P. Kim, Z.-Y. Li, L. V. Wang, Y. Liu and Y. Xia, *ACS Nano*, 2013, **7**, 2068-2077.
77. F. Zhou, S. Wu, S. Song, W. R. Chen, D. E. Resasco and D. Xing, *Biomaterials*, 2012, **33**, 3235-3242.
78. X. Wang, C. Wang, L. Cheng, S.-T. Lee and Z. Liu, *J. Am. Chem. Soc.*, 2012, **134**, 7414-7422.
79. L. Wang, J. Shi, H. Zhang, H. Li, Y. Gao, Z. Wang, H. Wang, L. Li, C. Zhang, C. Chen, Z. Zhang and Y. Zhang, *Biomaterials*, 2013, **34**, 262-274.

80. Y. Hashida, H. Tanaka, S. Zhou, S. Kawakami, F. Yamashita, T. Murakami, T. Umeyama, H. Imahori and M. Hashida, *J. Control. Release*, 2014, **173**, 59-66.
81. A. L. Antaris, J. T. Robinson, O. K. Yaghi, G. Hong, S. Diao, R. Luong and H. Dai, *ACS Nano*, 2013, **7**, 3644-3652.
82. X. C. Qin, Z. Y. Guo, Z. M. Liu, W. Zhang, M. M. Wan and B. W. Yang, *J. Photochem. Photobiol. B-Biol.*, 2013, **120**, 156-162.
83. Y. Wang, K. Wang, J. Zhao, X. Liu, J. Bu, X. Yan and R. Huang, *J. Am. Chem. Soc.*, 2013, **135**, 4799-4804.
84. K. Yang, J. Wan, S. Zhang, B. Tian, Y. Zhang and Z. Liu, *Biomaterials*, 2012, **33**, 2206-2214.
85. J. T. Robinson, S. M. Tabakman, Y. Liang, H. Wang, H. S. Casalongue, V. Daniel and H. Dai, *J. Am. Chem. Soc.*, 2011, **133**, 6825-6831.
86. O. Akhavan and E. Ghaderi, *Small*, 2013, **9**, 3593-3601.
87. O. Akhavan, E. Ghaderi, S. Aghayee, Y. Fereydooni and A. Talebi, *J. Mater. Chem.*, 2012, **22**, 13773-13781.
88. W. S. Seo, J. H. Lee, X. M. Sun, Y. Suzuki, D. Mann, Z. Liu, M. Terashima, P. C. Yang, M. V. McConnell, D. G. Nishimura and H. J. Dai, *Nat. Mater.*, 2006, **5**, 971-976.
89. S. Sherlock and H. Dai, *Nano Res.*, 2011, **4**, 1248-1260.
90. J. Yu, D. Javier, M. A. Yaseen, N. Nitin, R. Richards-Kortum, B. Anvari and M. S. Wong, *J. Am. Chem. Soc.*, 2010, **132**, 1929-1938.
91. J. Yang, J. Choi, D. Bang, E. Kim, E.-K. Lim, H. Park, J.-S. Suh, K. Lee, K.-H. Yoo, E.-K. Kim, Y.-M. Huh and S. Haam, *Angew. Chem. Int. Ed.*, 2011, **50**, 441-444.
92. L. Cheng, W. He, H. Gong, C. Wang, Q. Chen, Z. Cheng and Z. Liu, *Adv. Funct. Mater.*, 2013, **23**, 5893-5902.
93. C. Yue, P. Liu, M. Zheng, P. Zhao, Y. Wang, Y. Ma and L. Cai, *Biomaterials*, 2013, **34**, 6853-6861.
94. M. Zhou, R. Zhang, M. A. Huang, W. Lu, S. L. Song, M. P. Melancon, M. Tian, D. Liang and C. Li, *J. Am. Chem. Soc.*, 2010, **132**, 15351-15358.
95. C. M. Hessel, V. P. Pattani, M. Rasch, M. G. Panthani, B. Koo, J. W. Tunnell and B. A. Korgel, *Nano Lett.*, 2011, **11**, 2560-2566.
96. Q. Tian, F. Jiang, R. Zou, Q. Liu, Z. Chen, M. Zhu, S. Yang, J. Wang, J. Wang and J. Hu, *ACS Nano*, 2011, **5**, 9761-9771.
97. Z. Chen, Q. Wang, H. Wang, L. Zhang, G. Song, L. Song, J. Hu, H. Wang, J. Liu, M. Zhu and D. Zhao, *Adv. Mater.*, 2013, **25**, 2095-2100.
98. L. Cheng, J. Liu, X. Gu, H. Gong, X. Shi, T. Liu, C. Wang, X. Wang, G. Liu, H. Xing, W. Bu, B. Sun and Z. Liu, *Adv. Mater.*, 2014, **26**, 1886-1893.
99. M. C. DeRosa and R. J. Crutchley, *Coord. Chem. Rev.*, 2002, **233**, 351-371.
100. Y. N. Konan, R. Gurny and E. Allemann, *J. Photochem. Photobiol. B-Biol.*, 2002, **66**, 89-106.
101. Y. N. Konan, M. Berton, R. Gurny and E. Allemann, *Eur. J. Pharm. Sci.*, 2003, **18**, 241-249.
102. E. Allemann, N. Brasseur, O. Benrezzak, J. Rousseau, S. V. Kudrevich, R. W. Boyle, J. C. Leroux, R. Gurny and J. E. Vanlier, *J. Pharm. Pharmacol.*, 1995, **47**, 382-387.
103. Y. N. Konan-Kouakou, R. Boch, R. Gurny and E. Allemann, *J. Control. Release*, 2005, **103**, 83-91.
104. I. Roy, T. Y. Ohulchanskyy, H. E. Pudavar, E. J. Bergey, A. R. Oseroff, J. Morgan, T. J. Dougherty and P. N. Prasad, *J. Am. Chem. Soc.*, 2003, **125**, 7860-7865.
105. J. Dillon, J. C. Kennedy, R. H. Pottier and J. E. Roberts, *Photochem. Photobiol.*, 1988, **48**, 235-238.
106. D. K. Chatterjee, L. S. Fong and Y. Zhang, *Adv. Drug Deliv. Rev.*, 2008, **60**, 1627-1637.
107. I. Roy, T. Y. Ohulchanskyy, H. E. Pudavar, E. J. Bergey, A. R. Oseroff, J. Morgan, T. J. Dougherty and P. N. Prasad, *J. Am. Chem. Soc.*, 2003, **125**, 7860-7865.
108. V. Simon, C. Devaux, A. Darmon, T. Donnet, E. Thienot, M. Germain, J. Honnorat, A. Duval, A. Pottier, E. Borghi, L. Levy and J. Marill, *Photochem. Photobiol.*, 2010, **86**, 213-222.
109. S. Kim, T. Y. Ohulchanskyy, D. Bharali, Y. Chen, R. K. Pandey and P. N. Prasad, *J. Phys. Chem. C*, 2009, **113**, 12641-12644.
110. T. Y. Ohulchanskyy, I. Roy, L. N. Goswami, Y. Chen, E. J. Bergey, R. K. Pandey, A. R. Oseroff and P. N. Prasad, *Nano Lett.*, 2007, **7**, 2835-2842.
111. G. Charron, T. Stuchinskaya, D. R. Edwards, D. A. Russell and T. Nann, *J. Phys. Chem. C*, 2012, **116**, 9334-9342.
112. P. Juzenas, W. Chen, Y.-P. Sun, M. A. N. Coelho, R. Generalov, N. Generalova and I. L. Christensen, *Adv. Drug Deliv. Rev.*, 2008, **60**, 1600-1614.
113. S. J. Cho, D. Maysinger, M. Jain, B. Roder, S. Hackbarth and F. M. Winnik, *Langmuir*, 2007, **23**, 1974-1980.
114. P. Juzenas, R. Generalov, A. Juzeniene and J. Moan, *J. Biomed. Nanotechnol.*, 2008, **4**, 450-456.
115. V. Morosini, T. Bastogne, C. Frochot, R. Schneider, A. Francois, F. Guillemain and M. Barberi-Heyob, *Photochem. Photobiol. Sci.*, 2011, **10**, 842-851.
116. R. Bakalova, H. Ohba, Z. Zhelev, M. Ishikawa and Y. Baba, *Nat. Biotechnol.*, 2004, **22**, 1360-1361.
117. A. C. S. Samia, S. Dayal and C. Burda, *Photochem. Photobiol.*, 2006, **82**, 617-625.
118. A. Anas, H. Akita, H. Harashima, T. Itoh, M. Ishikawa and V. Biju, *J. Phys. Chem. B*, 2008, **112**, 10005-10011.
119. J. G. Liang, Z. K. He, S. S. Zhang, S. Huang, X. P. Ai, H. X. Yang and H. Y. Han, *Talanta*, 2007, **71**, 1675-1678.
120. A. C. S. Samia, X. Chen and C. Burda, *J. Am. Chem. Soc.*, 2003, **125**, 15736-15737.
121. R. Bakalova, H. Ohba, Z. Zhelev, T. Nagase, R. Jose, M. Ishikawa and Y. Baba, *Nano Lett.*, 2004, **4**, 1567-1573.
122. R. Rotomskis, J. Valanciunaite, A. Skripka, S. Steponkiene, G. Spogis, S. Bagdonas and G. Streckyte, *Lith. J. Phys.*, 2013, **53**, 57-68.
123. Z. D. Qi, D. W. Li, P. Jiang, F. L. Jiang, Y. S. Li, Y. Liu, W. K. Wong and K. W. Cheah, *J. Mater. Chem.*, 2011, **21**, 2455-2458.
124. C. Y. Hsu, C. W. Chen, H. P. Yu, Y. F. Lin and P. S. Lai, *Biomaterials*, 2013, **34**, 1204-1212.
125. K. L. Chou, H. Meng, Y. Cen, L. Li and J. Y. Chen, *J. Nanopart. Res.*, 2013, **15**, 1348.
126. C. Wang, L. Cheng and Z. Liu, *Theranostics*, 2013, **3**, 317-330.
127. P. Zhang, W. Steelant, M. Kumar and M. Scholfield, *J. Am. Chem. Soc.*, 2007, **129**, 4526-4527.
128. D. K. Chatterjee, M. K. Gnanasammandhan and Y. Zhang, *Small*, 2010, **6**, 2781-2795.
129. M. E. Lim, Y. L. Lee, Y. Zhang and J. J. H. Chu, *Biomaterials*, 2012, **33**, 1912-1920.
130. C. Wang, H. Q. Tao, L. Cheng and Z. Liu, *Biomaterials*, 2011, **32**, 6145-6154.
131. Y. Park, H. M. Kim, J. H. Kim, K. C. Moon, B. Yoo, K. T. Lee, N. Lee, Y. Choi, W. Park, D. Ling, K. Na, W. K. Moon, S. H. Choi, H. S. Park, S. Y.

- Yoon, Y. D. Suh, S. H. Lee and T. Hyeon, *Adv. Mater.*, 2012, **24**, 5755-5761.
132. X. H. Huang, I. H. El-Sayed, W. Qian and M. A. El-Sayed, *J. Am. Chem. Soc.*, 2006, **128**, 2115-2120.
133. B. Jang, J. Y. Park, C. H. Tung, I. H. Kim and Y. Choi, *ACS Nano*, 2011, **5**, 1086-1094.
134. S. J. Wang, P. Huang, L. M. Nie, R. J. Xing, D. B. Liu, Z. Wang, J. Lin, S. H. Chen, G. Niu, G. M. Lu and X. Y. Chen, *Adv. Mater.*, 2013, **25**, 3055-3061.
135. J. Lin, S. Wang, P. Huang, Z. Wang, S. Chen, G. Niu, W. Li, J. He, D. Cui, G. Lu, X. Chen and Z. Nie, *ACS Nano*, 2013, **7**, 5320-5329.
136. L. Li, M. Nurunnabi, M. Nafiujjaman, Y.-k. Lee and K. M. Huh, *J. Control. Release*, 2013, **171**, 241-250.
137. X. Huang, X.-J. Tian, W.-I. Yang, B. Ehrenberg and J.-Y. Chen, *Phys. Chem. Chem. Phys.*, 2013, **15**, 15727-15733.
138. L. Gao, J. Fei, J. Zhao, H. Li, Y. Cui and J. Li, *ACS Nano*, 2012, **6**, 8030-8040.
139. F. Li, S.-J. Park, D. Ling, W. Park, J. Y. Han, K. Na and K. Char, *J. Mater. Chem. B*, 2013, **1**, 1678-1686.
140. A. Sahu, W. I. Choi, J. H. Lee and G. Tae, *Biomaterials*, 2013, **34**, 6239-6248.
141. C. Fowley, N. Nomikou, A. P. McHale, B. McCaughan and J. F. Callan, *Chem. Commun.*, 2013, **49**, 8934-8936.
142. P. Huang, J. Lin, X. Wang, Z. Wang, C. Zhang, M. He, K. Wang, F. Chen, Z. Li, G. Shen, D. Cui and X. Chen, *Adv. Mater.*, 2012, **24**, 5104-5110.
143. K. Kano, Y. Tanaka, T. Ogawa, M. Shimomura, Y. Okahata and T. Kunitake, *Chem. Lett.*, 1980, 421-424.
144. R. H. Bisby, C. Mead and C. C. Morgan, *Biochem. Biophys. Res. Commun.*, 2000, **276**, 169-173.
145. G. Wang, X. Tong and Y. Zhao, *Macromolecules*, 2004, **37**, 8911-8917.
146. Y. Zhao, *Chem Rec*, 2007, **7**, 286-294.
147. C. Alvarez-Lorenzo, S. Deshmukh, L. Bromberg, T. A. Hatton, I. Sández-Macho and A. Concheiro, *Langmuir*, 2007, **23**, 11475-11481.
148. Y. Wang, P. Han, H. Xu, Z. Wang, X. Zhang and A. V. Kabanov, *Langmuir*, 2009, **26**, 709-715.
149. S. Angelos, E. Choi, F. Vögtle, L. De Cola and J. I. Zink, *J. Phys. Chem. C*, 2007, **111**, 6589-6592.
150. J. Lu, E. Choi, F. Tamanoi and J. I. Zink, *Small*, 2008, **4**, 421-426.
151. J. Liu, W. Bu, L. Pan and J. Shi, *Angew. Chem. Int. Ed.*, 2013, **52**, 4375-4379.
152. D. P. Ferris, Y.-L. Zhao, N. M. Khashab, H. A. Khatib, J. F. Stoddart and J. I. Zink, *J. Am. Chem. Soc.*, 2009, **131**, 1686-1688.
153. C.-J. Chen, G.-Y. Liu, X.-S. Liu, D.-D. Li and J. Ji, *New J. Chem.*, 2012, **36**, 694-701.
154. K. Peng, I. Tomatsu and A. Kros, *Chem. Commun.*, 2010, **46**, 4094-4096.
155. C. Wu, C. Chen, J. Lai, J. Chen, X. Mu, J. Zheng and Y. Zhao, *Chem. Commun.*, 2008, 2662-2664.
156. C. Park, K. Lee and C. Kim, *Angew. Chem. Int. Ed.*, 2009, **48**, 1275-1278.
157. N. K. Mal, M. Fujiwara and Y. Tanaka, *Nature*, 2003, **421**, 350-353.
158. H. M. Lin, W. K. Wang, P. A. Hsiung and S. G. Shyu, *Acta Biomater.*, 2010, **6**, 3256-3263.
159. S. Kumar, J.-F. Allard, D. Morris, Y. L. Dory, M. Lepage and Y. Zhao, *J. Mater. Chem.*, 2012, **22**, 7252-7257.
160. Y. Ma, X. Liang, S. Tong, G. Bao, Q. Ren and Z. Dai, *Adv. Funct. Mater.*, 2013, **23**, 815-822.
161. D. V. Volodkin, A. G. Skirtach and H. Möhwald, *Angew. Chem. Int. Ed.*, 2009, **48**, 1807-1809.
162. J. Yang, D. Shen, L. Zhou, W. Li, X. Li, C. Yao, R. Wang, A. M. El-Toni, F. Zhang and D. Zhao, *Chem. Mater.*, 2013, **25**, 3030-3037.
163. X. Yang, X. Liu, Z. Liu, F. Pu, J. Ren and X. Qu, *Adv. Mater.*, 2012, **24**, 2890-2895.
164. A. Barhoumi, R. Huschka, R. Bardhan, M. W. Knight and N. J. Halas, *Chem. Phys. Lett.*, 2009, **482**, 171-179.
165. E. Aznar, M. D. Marcos, R. Martinez-Manez, F. Sancenon, J. Soto, P. Amoros and C. Guillem, *J. Am. Chem. Soc.*, 2009, **131**, 6833-6843.
166. N. Fomina, J. Sankaranarayanan and A. Almutairi, *Adv. Drug Deliv. Rev.*, 2012, **64**, 1005-1020.
167. P. K. Selbo, A. Weyergang, A. Høgset, O.-J. Norum, M. B. Berstad, M. Vikdal and K. Berg, *J. Control. Release*, 2010, **148**, 2-12.
168. S. Febvay, D. M. Marini, A. M. Belcher and D. E. Clapham, *Nano Lett.*, 2010, **10**, 2211-2219.
169. C. Chen, L. Zhou, J. Geng, J. Ren and X. Qu, *Small*, 2013, **9**, 2793-2800.
170. R. Weissleder and M. J. Pittet, *Nature*, 2008, **452**, 580-589.
171. L. Bu, X. Ma, Y. Tu, B. Shen and Z. Cheng, *Curr. Pharm. Biotechnol.*, 2014, **14**, 723-732.
172. A. Srivatsan, S. V. Jenkins, M. Jeon, Z. Wu, C. Kim, J. Chen and R. K. Pandey, *Theranostics*, 2014, **4**, 163-174.
173. Y. Huang, S. He, W. Cao, K. Cai and X.-J. Liang, *Nanoscale*, 2012, **4**, 6135-6149.
174. J. Shen, L. Zhao and G. Han, *Adv. Drug Deliv. Rev.*, 2013, **65**, 744-755.
175. S.-H. Hu, Y.-W. Chen, W.-T. Hung, I. W. Chen and S.-Y. Chen, *Adv. Mater.*, 2012, **24**, 1748-1754.
176. A. M. Derfus, G. von Maltzahn, T. J. Harris, T. Duza, K. S. Vecchio, E. Ruoslahti and S. N. Bhatia, *Adv. Mater.*, 2007, **19**, 3932-3936.
177. J. Yu, D.-Y. Huang, Y. Muhammad Zubair, Y.-L. Hou and S. Gao, *Chin. Phys. B*, 2013, **22**, 027506.
178. S. Sharifi, S. Behzadi, S. Laurent, M. Laird Forrest, P. Stroeve and M. Mahmoudi, *Chem. Soc. Rev.*, 2012, **41**, 2323-2343.
179. J. Dobson, *Gene Ther.*, 2006, **13**, 283-287.
180. S. F. Medeiros, A. M. Santos, H. Fessi and A. Elaissari, *Int. J. Pharm.*, 2011, **403**, 139-161.
181. L. Cheng, K. Yang, Y. Li, X. Zeng, M. Shao, S.-T. Lee and Z. Liu, *Biomaterials*, 2012, **33**, 2215-2222.
182. Y. Zhou, Z. Tang, C. Shi, S. Shi, Z. Qian and S. Zhou, *J. Mater. Sci. - Mater. Med.*, 2012, **23**, 2697-2708.
183. C. Huettinger, J. Hirschberger, A. Jahnke, R. Koestlin, T. Brill, C. Plank, H. Kuechenhoff, S. Krieger and U. Schillinger, *J. Gene. Med.*, 2008, **10**, 655-667.
184. T. T. T. N'Guyen, H. T. T. Duong, J. Basuki, V. Montembault, S. Pascual, C. Guibert, J. Fresnais, C. Boyer, M. R. Whittaker, T. P. Davis and L. Fontaine, *Angew. Chem. Int. Ed.*, 2013, **52**, 14152-14156.
185. R. Li, R. a. Wu, L. Zhao, M. Wu, L. Yang and H. Zou, *ACS Nano*, 2010, **4**, 1399-1408.
186. S.-H. Hu, Y.-Y. Chen, T.-C. Liu, T.-H. Tung, D.-M. Liu and S.-Y. Chen, *Chem. Commun.*, 2011, **47**, 1776-1778.
187. Y.-J. Kim, M. Ebara and T. Aoyagi, *Adv. Funct. Mater.*, 2013, **23**, 5753-5761.
188. T.-Y. Liu, K.-H. Liu, D.-M. Liu, S.-Y. Chen and I. W. Chen, *Adv. Funct. Mater.*, 2009, **19**, 616-623.

- 189.C. R. Thomas, D. P. Ferris, J.-H. Lee, E. Choi, M. H. Cho, E. S. Kim, J. F. Stoddart, J.-S. Shin, J. Cheon and J. I. Zink, *J. Am. Chem. Soc.*, 2010, **132**, 10623-10625.
- 190.D. Yoo, J.-H. Lee, T.-H. Shin and J. Cheon, *Acc. Chem. Res.*, 2011, **44**, 863-874.
- 191.J. Lim and J. Dobson, *J. Genet.*, 2012, **91**, 223-227.
- 192.C. Plank, O. Zelphati and O. Mykhaylyk, *Adv. Drug Deliv. Rev.*, 2011, **63**, 1300-1331.
- 193.D. Yoo, H. Jeong, S.-H. Noh, J.-H. Lee and J. Cheon, *Angew. Chem. Int. Ed.*, 2013, **52**, 13047-13051.
- 194 L.-Y. Zhao, J.-Y. Liu, W.-W. Ouyang, D.-Y. Li, L. Li, L.-Y. Li and J.-T. Tang, *Chin. Phys. B*, 2013, **22**, 108104.
- 195.G. Nedelcu, *Dig. J. Nanomater. Biostruct.*, 2008, **3**, 103-107.
- 196.N. K. Prasad, K. Rathinasamy, D. Panda and D. Bahadur, *J. Mater. Chem.*, 2007, **17**, 5042-5051.
- 197.K. H. Bae, M. Park, M. J. Do, N. Lee, J. H. Ryu, G. W. Kim, C. Kim, T. G. Park and T. Hyeon, *ACS Nano*, 2012, **6**, 5266-5273.
- 198.A. Ito, M. Shinkai, H. Honda and T. Kobayashi, *Cancer Gene Ther.*, 2001, **8**, 649-654.
- 199.H. L. Rodriguez-Luccioni, M. Latorre-Esteves, J. Mendez-Vega, O. Soto, A. R. Rodriguez, C. Rinaldi and M. Torres-Lugo, *Int. J. Nanomed.*, 2011, **6**, 373-380.
- 200.I. Marcos-Campos, L. Asin, T. E. Torres, C. Marquina, A. Tres, M. R. Ibarra and G. F. Goya, *Nanotechnology*, 2011, **22**, 205101.
- 201.L. Asin, M. Ibarra, A. Tres and G. Goya, *Pharm. Res.*, 2012, **29**, 1319-1327.
- 202.P. Guardia, R. Di Corato, L. Lartigue, C. Wilhelm, A. Espinosa, M. Garcia-Hernandez, F. Gazeau, L. Manna and T. Pellegrino, *ACS Nano*, 2012, **6**, 3080-3091.
- 203.M. Colombo, S. Carregal-Romero, M. F. Casula, L. Gutierrez, M. P. Morales, I. B. Boehm, J. T. Heverhagen, D. Prospero and W. J. Parak, *Chem. Soc. Rev.*, 2012, **41**, 4306-4334.
- 204.A. Ito, M. Shinkai, H. Honda, T. Wakabayashi, J. Yoshida and T. Kobayashi, *Cancer Immunol Immunother*, 2001, **50**, 515-522.
- 205.J.-t. Jang, H. Nah, J.-H. Lee, S. H. Moon, M. G. Kim and J. Cheon, *Angew. Chem. Int. Ed.*, 2009, **48**, 1234-1238.
- 206.R. E. Rosensweig, *J. Magn. Magn. Mater.*, 2002, **252**, 370-374.
- 207.E. Kita, T. Oda, T. Kayano, S. Sato, M. Minagawa, H. Yanagihara, M. Kishimoto, C. Mitsumata, S. Hashimoto, K. Yamada and N. Ohkohchi, *J. Phys. D: Appl. Phys.*, 2010, **43**, 474011.
- 208.R. M. Patil, P. B. Shete, N. D. Thorat, S. V. Otari, K. C. Barick, A. Prasad, R. S. Ningthoujam, B. M. Tiwale and S. H. Pawar, *J. Magn. Magn. Mater.*, 2014, **355**, 22-30.
- 209.R. Hao, J. Yu, Z. Ge, L. Zhao, F. Sheng, L. Xu, G. Li and Y. Hou, *Nanoscale*, 2013, **5**, 11954-11963.
- 210.J. Shin, C.-H. Yoo, J. Lee and M. Cha, *Biomaterials*, 2012, **33**, 5650-5657.
- 211.C.-A. M. Smith, J. d. l. Fuente, B. Pelaz, E. P. Furlani, M. Mullin and C. C. Berry, *Biomaterials*, 2010, **31**, 4392-4400.
- 212.P. Hinterdorfer, W. Baumgartner, H. J. Gruber, K. Schilcher and H. Schindler, *Proc. Natl. Acad. Sci. U. S. A.*, 1996, **93**, 3477-3481.
- 213.S. B. Smith, Y. Cui and C. Bustamante, *Science*, 1996, **271**, 795-799.
- 214.S. I. Lee, K. H. Park, S. J. Kim, Y. G. Kang, Y. M. Lee and E. C. Kim, *Clin. Exp. Immunol.*, 2012, **168**, 113-124.
- 215.N. Wang, J. Butler and D. Ingber, *Science*, 1993, **260**, 1124-1127.
- 216.J.-H. Lee, E. S. Kim, M. H. Cho, M. Son, S.-I. Yeon, J.-S. Shin and J. Cheon, *Angew. Chem. Int. Ed.*, 2010, **49**, 5698-5702.
- 217.M. H. Cho, E. J. Lee, M. Son, J.-H. Lee, D. Yoo, J.-w. Kim, S. W. Park, J.-S. Shin and J. Cheon, *Nat. Mater.*, 2012, **11**, 1038-1043.
- 218.S.-H. Hu and X. Gao, *J. Am. Chem. Soc.*, 2010, **132**, 7234-7237.
- 219.J. Kim, H. S. Kim, N. Lee, T. Kim, H. Kim, T. Yu, I. C. Song, W. K. Moon and T. Hyeon, *Angew. Chem. Int. Ed.*, 2008, **47**, 8438-8441.
- 220.Y. Chang, N. Liu, L. Chen, X. Meng, Y. Liu, Y. Li and J. Wang, *J. Mater. Chem.*, 2012, **22**, 9594-9601.
- 221.R. Xing, G. Liu, Q. Quan, A. Bhirde, G. Zhang, A. Jin, L. H. Bryant, A. Zhang, A. Liang, H. S. Eden, Y. Hou and X. Chen, *Chem. Commun.*, 2011, **47**, 12152-12154.
- 222.M. F. Kircher, A. de la Zerda, J. V. Jokerst, C. L. Zavaleta, P. J. Kempen, E. Mittra, K. Pitter, R. Huang, C. Campos, F. Habte, R. Sinclair, C. W. Brennan, I. K. Mellinshoff, E. C. Holland and S. S. Gambhir, *Nat. Med.*, 2012, **18**, 829-834.
- 223.J. Zeng, L. Jing, Y. Hou, M. Jiao, R. Qiao, Q. Jia, C. Liu, F. Fang, H. Lei and M. Gao, *Adv. Mater.*, 2014, **26**, 2694-2698.
- 224.R. McLaughlin and N. Hylton, *NMR Biomed.*, 2011, **24**, 712-720.
- 225.B. Qiu and X. Yang, *Nat. Clin. Pract. Cardiovasc. Med.*, 2008, **5**, 396-404.
- 226.Y. Guan, H.-B. Zhao, L.-X. Yu, S.-C. Chen and Y.-Z. Wang, *RSC Adv.*, 2014, **4**, 4955-4959.
- 227.D. Xiao, H.-Z. Jia, J. Zhang, C.-W. Liu, R.-X. Zhuo and X.-Z. Zhang, *Small*, 2014, **10**, 591-598.
- 228.S. Wu, X. Huang and X. Du, *Angew. Chem. Int. Ed.*, 2013, **52**, 5580-5584.
- 229.A. Curcio, R. Marotta, A. Riedinger, D. Palumberi, A. Falqui and T. Pellegrino, *Chem. Commun.*, 2012, **48**, 2400-2402.
- 230.S. Zhou, X. Du, F. Cui and X. Zhang, *Small*, 2014, **10**, 980-988.

TOC



Nanoparticles (NPs)-based stimuli-sensitive cancer therapy, including pH-, reduction-sensitive NPs and light-, magnetic field-responsive NPs are reviewed.